



Innovative modeling techniques including MEP, ANN and FQ to forecast the compressive strength of geopolymer concrete modified with nanoparticles

Hemn Unis Ahmed^{1,2} · Ahmed S. Mohammed¹ · Rabar H. Faraj³ · Aso A. Abdalla¹ · Shaker M. A. Qaidi^{4,6} · Nadhim Hamah Sor⁵ · Azad A. Mohammed¹

Received: 13 December 2021 / Accepted: 13 February 2023 / Published online: 1 March 2023
© The Author(s), under exclusive licence to Springer-Verlag London Ltd., part of Springer Nature 2023

Abstract

The use of nano-materials to improve the engineering properties of different types of concrete composites including geopolymer concrete (GPC) has recently gained popularity. Numerous programs have been executed to investigate the mechanical properties of GPC. In general, compressive strength (CS) is an essential mechanical indicator for judging the quality of concrete. Traditional test methods for determining the CS of GPC are expensive, time-consuming and limiting due to the complicated interplay of a wide variety of mixing proportions and curing regimes. Therefore, in this study, artificial neural network (ANN), multi-expression programming, full quadratic, linear regression and M5P-tree machine learning techniques were used to predict the CS of GPC. In this instance, around 207 tested CS values were extracted from the literature and studied to promote the models. During the process of modeling, eleven effective variables were utilized as input model parameters, and one variable was utilized as an output. Four statistical indicators were used to judge how well the models worked, and the sensitivity analysis was carried out. According to the results, the ANN model calculated the CS of GPC with greater precision than the other models. On the other hand, the ratio of alkaline solution to the binder, molarity, NaOH content, curing temperature and concrete age have substantial effects on the CS of GPC.

Keywords Geopolymer concrete · Modeling · Compressive strength · Artificial neural network · Multi-expression programming · Sensitivity analysis

1 Introduction

Concrete, after water, is the second most often used substance on the earth, and it demands massive quantities of Portland cement (PC). The production of PC necessitates a huge amount of natural resources, such as limestone and fossil fuels, but it also produces roughly 0.8 tonnes of CO₂ per tonne of cement clinker produced [1, 2]. The cement industry is second regarding how much CO₂ it puts into the air. Compared to what they are right now, CO₂ emissions are expected to reach a peak of 100% by 2020. By 2050, the world will make 4.38 billion tons of cement each year, which is a 5% increase every year [3, 4]. Because of this, all countries have to think about CO₂ emission regulations and reductions [5]. In response to the expanding sources of solid waste and the need to minimize climate change, the most pressing issue in modern material science is discovering and innovating new sustainable and environmentally

✉ Hemn Unis Ahmed
hemn.ahmed@univsul.edu.iq

¹ Civil Engineering Department, University of Sulaimani, College of Engineering, Sulaimaniyah, Kurdistan Region, Iraq

² Civil Engineering Department, Komar University of Science and Technology, Sulaimani, Kurdistan Region, Iraq

³ Civil Engineering Department, University of Halabja, Halabja, Kurdistan Region, Iraq

⁴ Civil Engineering Department, College of Engineering, University of Duhok, Duhok, Kurdistan Region, Iraq

⁵ Civil Engineering Department, University of Garmian, Kalar, Kurdistan Region, Iraq

⁶ Department of Civil Engineering, College of Engineering, Nawroz University, 42001 Duhok, Iraq

friendly materials [6]. Consequently, substantial research has been performed to develop a new material that can be utilized as an alternative to Portland cement [7]; among them, geopolymer technology was developed in France by professor Davidovits [8].

Geopolymers are produced via a polymerization process involving the chemical interaction of alumina silicate minerals in the presence of an alkaline medium which results in the formation of a three-dimensional polymeric chain [9]. The mixed proportions of the GPC consist of aluminosilicate source binder materials, fine and coarse aggregates, alkaline solutions and sometimes extra water [10]. The polymerization between the alkaline solutions and source binder materials produces solid concrete, almost like traditional binder concrete composites [11]. Many factors influence on the properties and performances of GPC, including the molarity of NaOH, the ratio of Na_2SiO_3 to NaOH, curing regime and ages, water-to-solid ratio, alkaline solution-to-binder ratio, elemental composition and type of source binder materials, ratio of Si to Al in the geopolymer system, mixing time and rest period, superplasticizer dosage and extra water contents, and coarse and fine aggregate contents [12].

Nanotechnology is an emerging revolutionary discipline in civil engineering that is in its infancy. For GPC composites, nano-materials of various types offer substantial advantages over other additives, including superior mechanical properties and long-term durability [13]. Recent initiatives to introduce nanoparticles (NPs) into construction materials to improve the characteristics and performance of concrete have been made [14]. NPs were introduced with geopolymer matrices to enhance durability issues, physical structure and mechanical properties of the geopolymer mixture [15]. Because NPs have a higher surface area-to-volume ratio, they are highly reactive and have an effect on reaction rates [16]. As a result, NPs modifies the microstructure of GPC at the atomic level, resulting in significant improvements in both the fresh and hardened states and the microstructural behavior of geopolymer composites [17]. In the literature, a wide range of NPs like nano-silica (NS), nano-clay, nano-alumina, carbon nanotubes, nano-metakaolin and nano-titanium were consumed to improve various properties of the geopolymer composites, with NS being the most frequent [13]. This study was focused on presenting several methods to estimate the CS of GPC composites modified with NS, since nano-silica was the most widely employed material among all NP kinds.

When determining the overall quality of concrete, one of the most important mechanical parameters to look at is compressive strength (CS). Other mechanical and durability metrics are connected to CS and can be calculated based on their indirect correlations with CS [18]. To

figure out the CS of GPCs in real life, multiple cube and cylinder samples are made and tested at different curing times. Work on a construction site should not go on until a certain age, like 28 days, when the CS test results are known. This slows down building projects and makes the testing process time-consuming and expensive [19].

Because adjusting the mix proportions and components can have a substantial effect on the properties of GPC, estimating its CS without conducting trials has been one of the most challenging issues in concrete technology for a very long time [20].

With continued research into the CS for GPC, standard approaches for determining the CS for normal concrete may no longer be applicable to GPC mixtures. Some researchers attempted to use a regression equation to tie the variables to the CS of GPC. As CS is sensitive to the proportions of the mixture and depends on various characteristics, engineers should be provided with easier procedures and mathematical formulas to forecast the outcomes of experiments. Soft computing approaches could be considered a viable solution [21]. The best feature about these methods is that they may be used to generate alternatives and solutions for linear and nonlinear issues when mathematical models cannot effectively demonstrate how the problem's main aspects are related to one another [22].

Artificial intelligence systems for analyzing and forecasting the mechanical properties of cement-based materials are a hot topic in the cement-based composites research sector to provide the construction industry with new methodologies and strategies for application. Machine learning has developed as a potent method for determining structural and material performance. Machine learning models use a huge amount of acquired or measured actual data with features with a wide range of values, allowing such models to be extremely generalizable and resilient. Adaptive neuro-fuzzy inference systems were utilized by Bilir et al. [23] to forecast the width of constrained drying shrinkage cracks in slag mortar composites. The model allowed for effective steps to be adopted to prevent concrete cracking, resulting in increased concrete durability. The MSP model tree was used by Behnood and Daneshvar [24] to calculate the dynamic modulus of asphalt concrete. Ahmed et al. [25] successfully used twelve effective mixture proportions and curing conditions as the model input parameters to predict the CS of fly ash-based geopolymer concrete by adapting three common models: linear, non-linear and multi-logistic regression models.

Due to the limited test data and the number of side variables addressed, applying these empirical formulas to other scenarios is challenging. This necessitates the development of a novel method for accurately estimating the compressive strength of GPC, taking into account the

impact of various mixture proportions and curing ages. The above studies showed that machine learning techniques could perform excellently with many variables while overcoming drawbacks like a lack of experimental data and the inability to generalize the model to other contexts. Even though GPCs are used in many projects, there are not many studies on how to predict the CS of GPCs modified with nano-silica, so it is hard to use them quickly in the building industry. Also, the construction industry is looking more and more for new building materials with unique properties that can make concrete structures last longer. This means that new models need to be made to predict how these new materials will act. So, the main purpose of this study is to figure out how different mixture proportions affect the compression resistance of GPCs from a young age to a long-term curing age, including the alkaline solution-to-binder ratio (l/b), binder content (B), fine (FA) and coarse (CA) aggregate content, sodium hydroxide (SH) and sodium silicate (SS) content, the ratio of SS to SH, the molarity of SH (M), NS content, curing temperatures (T) and concrete ages (A). In the literature, there is a shortage of studies examining the impact of different mixture proportion parameters on the CS of GPC modified with NS at various curing temperatures and ages. Therefore, in this study, different model techniques, namely artificial neural network (ANN), multi-expression programming (MEP), full quadratic (FQ), linear regression (LR) and M5P-tree machine learning techniques, were used to predict the CS of GPC. Finally, different statistical tools, such as the root-mean-square error (RMSE), scatter index (SI), objective value (OBJ) and the correlation coefficient (R), were used to evaluate the created models' accuracy.

2 Aim of the study

The purpose of this work is to examine the use of the MEP, ANN, FQ, M5P and LR models to forecast the compressive strength of geopolymer concrete with or without nano-silica with the following aims:

- (i) Analyze the acquired data statistically to see how the mix proportion of GPC incorporated with nano-silica affects compressive strength.
- (ii) Develop a credible model to estimate the compressive strength of GPC enhanced with nano-silica and determine the models' sensitivity using various statistical methodologies.
- (iii) Provide the simplest formulae to be used by engineers and academics in their GPC mix design projects.

3 Methodology

In total, 207 experimental data from earlier studies were gathered and statistically evaluated before dividing into two groups. The first and more prominent group comprised 145 datasets utilized to create the models. Moreover, the remaining data (62 data) were utilized to test the models [26]. Table 1 summarizes the GPC mixes database and the measured CS of GPC produced with various mix proportions incorporated nS. Several databases' search portals, such as Google Scholar, Web of Science, Scopus and Science Direct, were utilized to conduct a comprehensive literature search as part of the database preparation process. The majority of prior studies discussing the effect of nS additions on the characteristics of GPCs were collected, and their data were retrieved based on the authors' searches.

Table 1 shows the input dataset, which includes: l/b ranges from 0.4 to 0.4, B ranges from 300 to 500 kg/m³, FA ranges from 490 to 990 kg/m³, CA ranges from 810 to 1470 kg/m³, SH ranges from 18.17 to 159.75 kg/m³, SS ranges from 40.8 to 187.5 kg/m³, M ranges from 4 to 16 M, SS/SH ranges from 0.33 to 3, NS ranges from 0 to 60 kg/m³, T ranges from 23 to 70 °C, A ranges from 0.5 to 180 days, and CS ranges from 3.2 to 81.3 MPa. The given dataset, which included those mentioned above eleven independent factors, was utilized to forecast the CS of GPC produced with different mixtures using several approaches compared to the measured reported CS (MPa). Figure 1 depicts the procedure used in this investigation in terms of a flowchart. In addition, the next parts describe and explain the specifics, such as data gathering, analysis, modeling and assessment.

4 Statistical assessment

In this part, a statistical study was performed to determine whether or not there are substantial correlations and histograms between input parameters and CS of GPCs. To do so, all input variables such as (i) alkaline solution-to-binder ratio (Fig. 2a), (ii) binder content (Fig. 2b), (iii) fine aggregate content (Fig. 2c), (iv) coarse aggregate content (Fig. 2d), (v) sodium hydroxide content (Fig. 2e), (vi) sodium silicate content (Fig. 2f), (vii) molarity (Fig. 2g), (viii) sodium silicate-to-sodium hydroxide ratio (Fig. 2h), (ix) nano-silica content (Fig. 2i), (x) curing temperature (Fig. 2j) and (xi) specimens age (Fig. 2k) were plotted and analyzed with actual CS; additionally, the normal distribution of obtained CS from previous studies is shown in the above figures. In addition, statistical functions such as minimum, maximum, average, standard deviation,

Table 1 Summary of the constituents of geopolymer concrete mixes reported in the literature

Ref	l/b	B (kg/m ³)	FA (kg/m ³)	CA (kg/m ³)	SH (kg/m ³)	SS (kg/m ³)	M	SS/SH	NS (kg/m ³)	T (°C)	A (days)	CS (MPa)
[17]	0.4	440	723	1085	64	112	12	1.75	0–26.4	28–60	3_28	21.7–46.43
[27]	0.45	362.8	990	810	122.4	40.8	4	0.33	0–10.88	25	7–120	35.5–61.8
[28]	0.45	500–460	790	907	62.5	187.5	12	2.33	0–40	28	7_28	29–48
[29]	0.45	486–490	490	1470	73	154	12	2	0–3.675	31.5	3_28	8.95–62.8
[30]	0.45	500	575	1150	64.3	160.7	14	2.5	0–15	70	30	51.63–42.71
[31]	0.45	393–414	692–684	1240–1233	46.6–44.2	139.7–132.6	4	3	0–20.7	23	28–60	52–76.5
[32]	0.6	450	500	970–1150	135	135	10	1	0–13.5	25	7_90	18.6–47.3
[33]	0.45	380.689	554.4	1295	48.945	122.364	8_16	2.5	0–5.71	60	28	38.1
[34]	0.52	370–400	650	1206	60	150	14	2.5	0–30	60	1_28	4.7–45
[35]	0.6	300	800	1200	85	95	12	1.1	0–9	25	7_28	18.9–45.9
[36]	0.5	339–350	720	1305	43.5–45	108.9–112.5	16	2.5	0–21	60	7_28	3.2–24.4
[37]	0.6	450	500	1036–1150	108	162	12	1.5	0–9	60	28	31.6–42.6
[38]	0.45	497	560	1120	159.75	63.9	12	0.4	0–49.7	60	28	24–35
[39]	0.5	450	750	1000	75	150	12	2	0–13.5	25	7_28	21.9–50.4
[40]	0.4	394.29	554.4	1293.6	45.06	112.64	12	2.5	0–3.94	24	28	44.3–48.6
[41]	0.45	450–500	825	825	18.17–28.57	144.65–160.75	10_16	2.5	0–10	60	7_90	41.1–81.3
[42]	0.52	370–400	620–650	1152–1206	60	150	14	2.5	0–60	24	3–180	4.3–61.2
[43]	0.45	405.8–413.8	888	945	53.2	133	12	2.5	0–8.3	29	28–90	37.1–52.3
[44]	0.52	370–400	620–650	1152–1206	60	150	14	2.5	0–60	60	0.5–28	4.9–45.1
Min	0.4	300	490	810	18.17	40.8	4	0.33	0	23	0.5	3.2
Max	0.6	500	990	1470	159.75	187.5	16	3	60	70	180	81.3
St.Div	0.1	51.9	135.3	183.3	33.9	35.6	3.3	0.8	14.6	17.4	31.8	17.5

*l/b = alkaline solution-to-binder ratio, B = binder content (kg/m³), FA = fine aggregate content (kg/m³), CA = coarse aggregate content (kg/m³), SH = sodium hydroxide content (kg/m³), SS = sodium silicate content (kg/m³), M = molarity (M), SS/SH = ratio of sodium silicate to sodium hydroxide, NS = nano-silica content (kg/m³), T = curing temperature (°C), A = age (days) and CS = actual compressive strength (MPa)

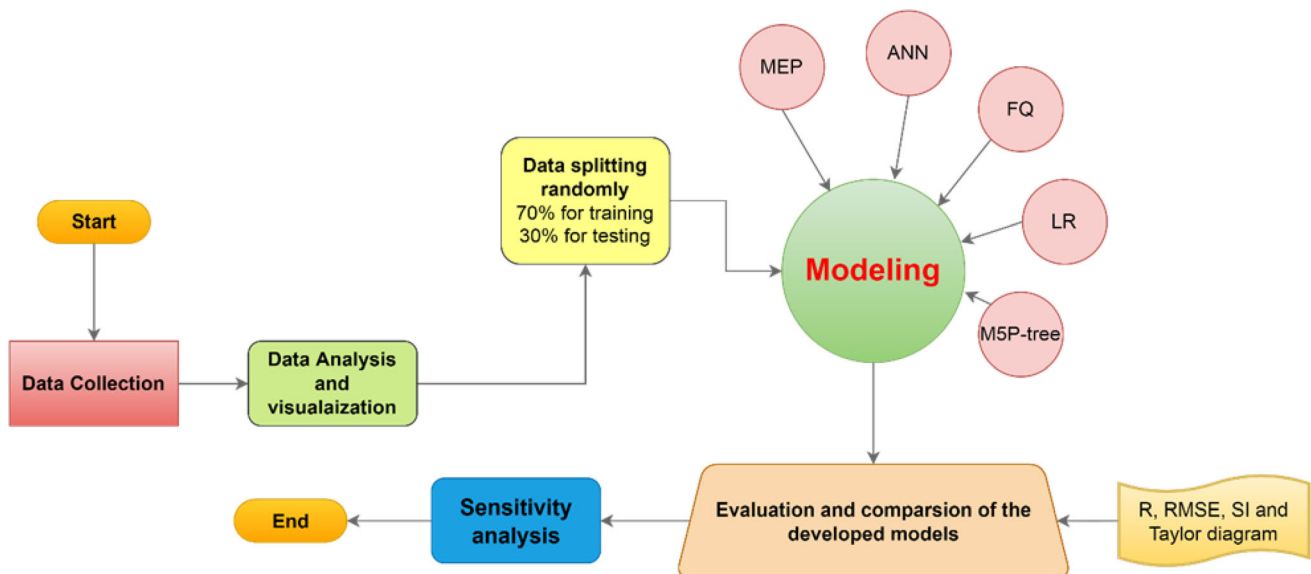
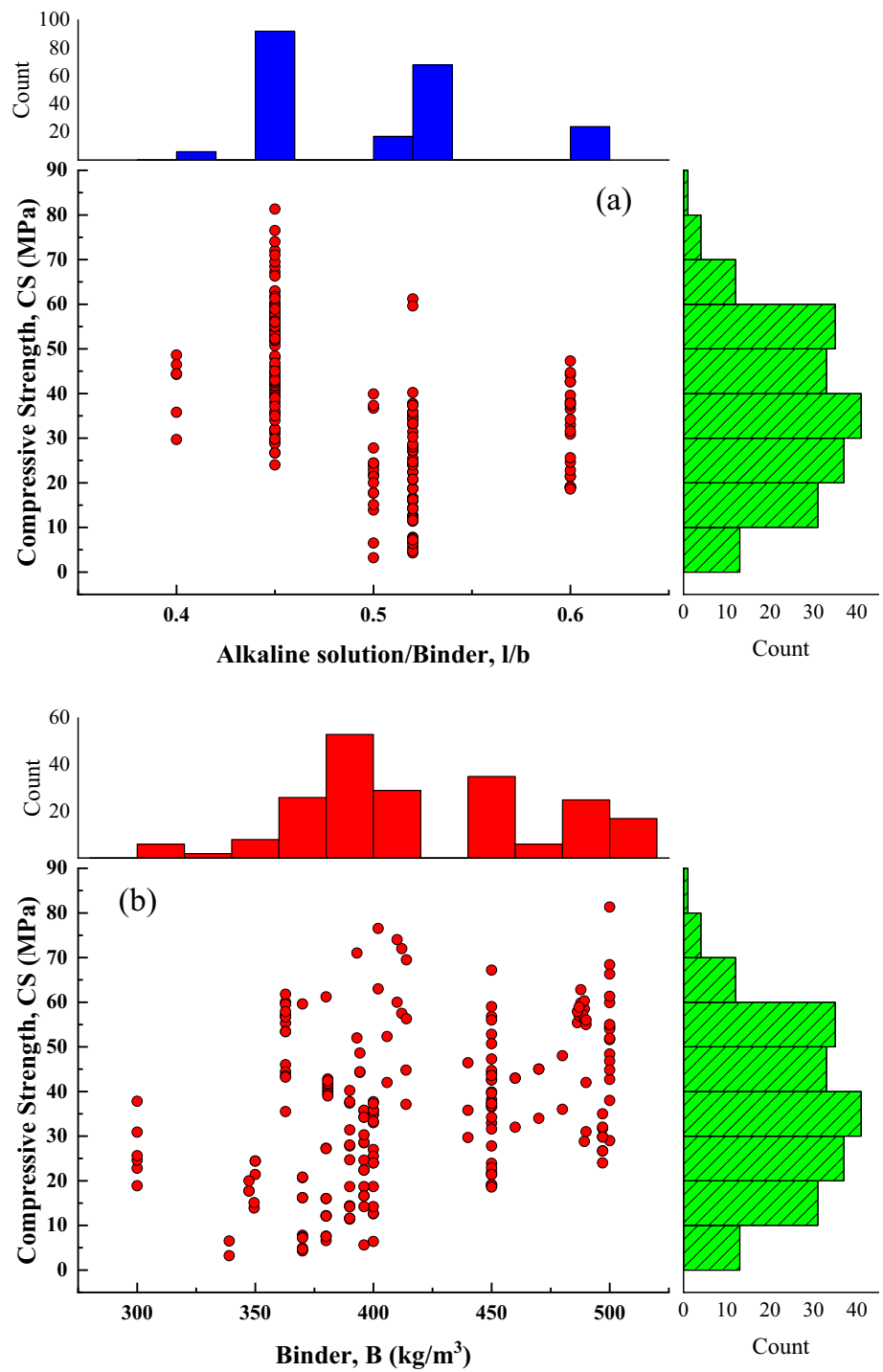


Fig. 1 Flowchart diagram process followed in this study

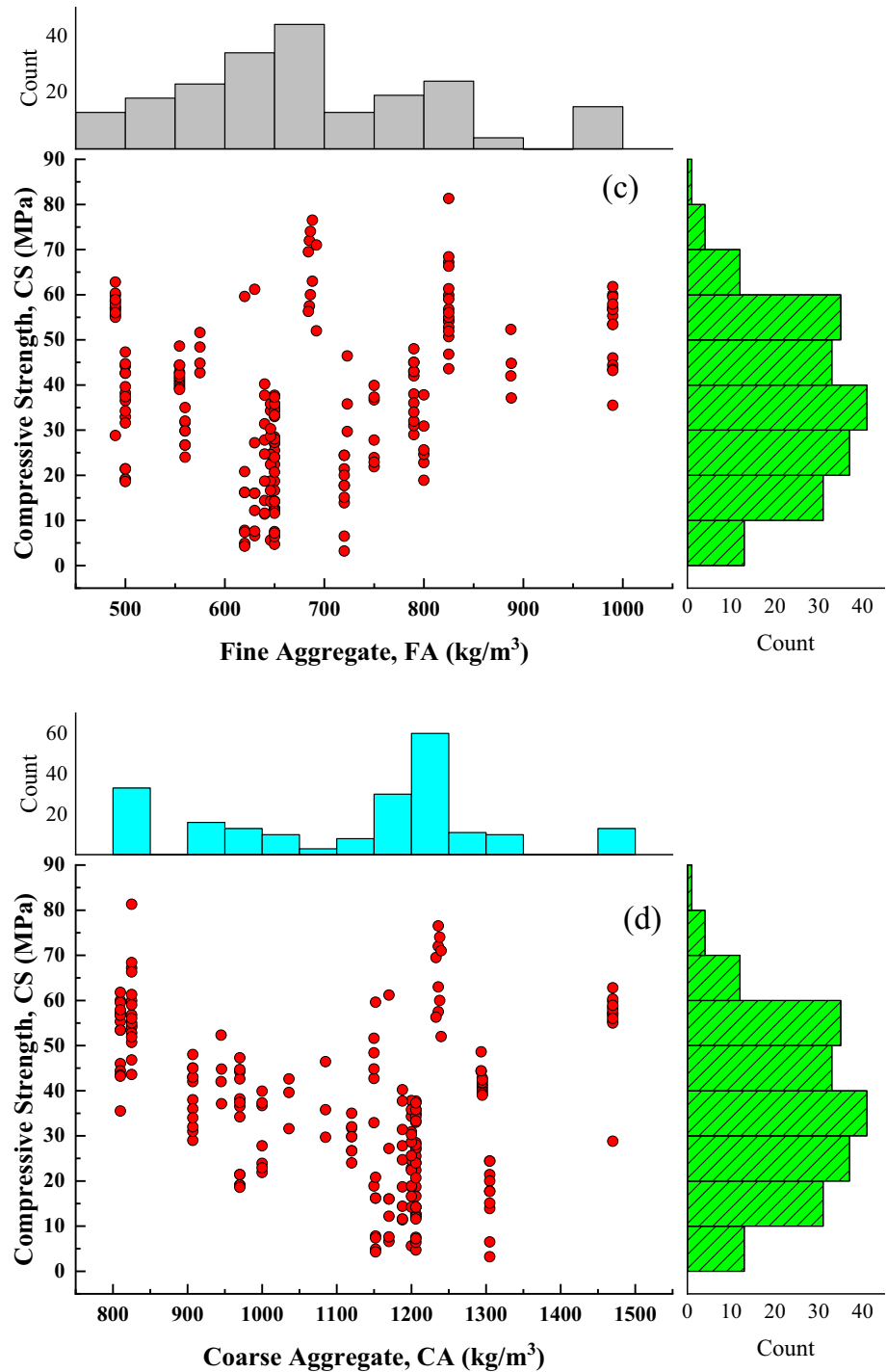
Fig. 2 Marginal plot for the CS of GPC mixtures incorporated nS versus: **a:** alkaline solution-to-binder ratio (*l/b*); **b:** binder content (*B*); **c:** fine aggregate content (*FA*); **d:** coarse aggregate content (*CA*); **e:** sodium hydroxide content (*SH*); **f:** sodium silicate content (*SS*); **g:** molarity of sodium hydroxide (*M*); **h:** sodium silicate-to-sodium hydroxide ratio (*SS/SH*); **i:** nano-silica content (*NS*); **j:** curing temperature (*T*); **k:** age of GPC specimens (*A*)



skewness, kurtosis and variance were calculated and are displayed in Table 2 to show the distribution of each variable. Regarding the kurtosis parameter, a high negative value represents the shorter tails relative to the normal distribution, and a positive value represents the longer tails. An immense negative value for the skewness parameter indicates a long-left tail, while a positive value indicates a right tail [45].

Based on the collected datasets, the ratio of *l/b* of the GPC mixtures modified with nS was in the range of 0.4 to 0.6, with the average and standard deviations of 0.49 and 0.05, respectively. Also, regarding other statistical analyses, it was found that the variance was 0.002, skewness was 0.66, and the kurtosis was -0.25 . The ranges of binders were between 300 and 500 kg/m³, with the average and standard deviations of 417 kg/m³ and 51.8 kg/m³,

Fig. 2 continued

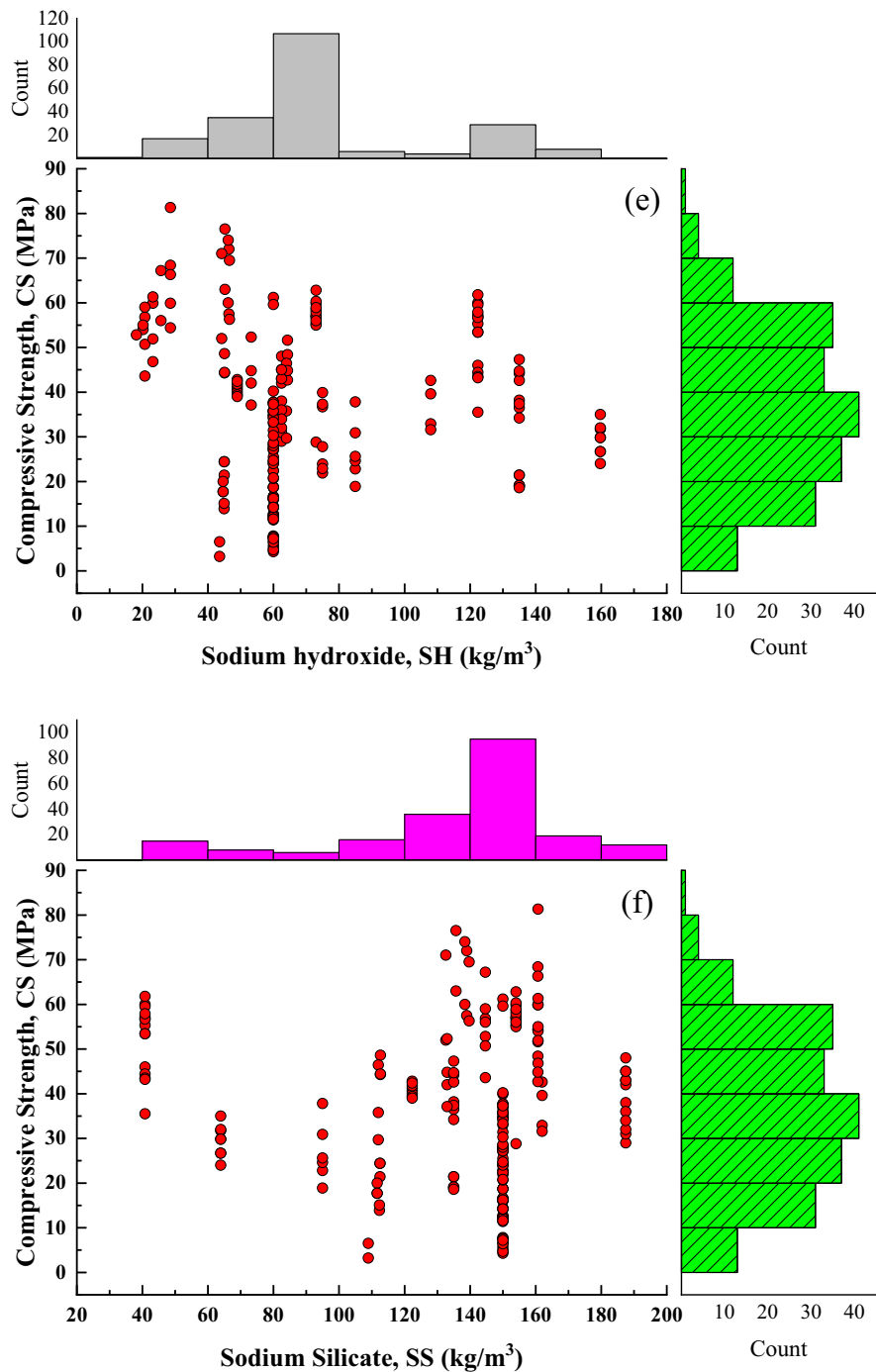


correspondingly. At the same time, other statistical assessment tools like variance, skewness and kurtosis were 2689, 0.11 and -0.81 , respectively.

Like traditional concrete mixtures, natural and crushed aggregates were used as the FA and CA in GPC mixtures. The FA should be satisfied with the requirements of ASTM standards. According to gathered datasets from the literature article, it was found that the range of FA was between

490 and 990 kg/m³, with an average of 681 kg/m³ and standard deviations of 135.2 kg/m³. Furthermore, regarding the ranges of CA, it was concluded that the contents of CA in past research varied between 810 and 1470 kg/m³ with an average of 1113.8 kg/m³ and standard deviations of 183.2 kg/m³. On the other hand, the variance, skewness and kurtosis were 33,580, -0.19 and -0.71 , respectively.

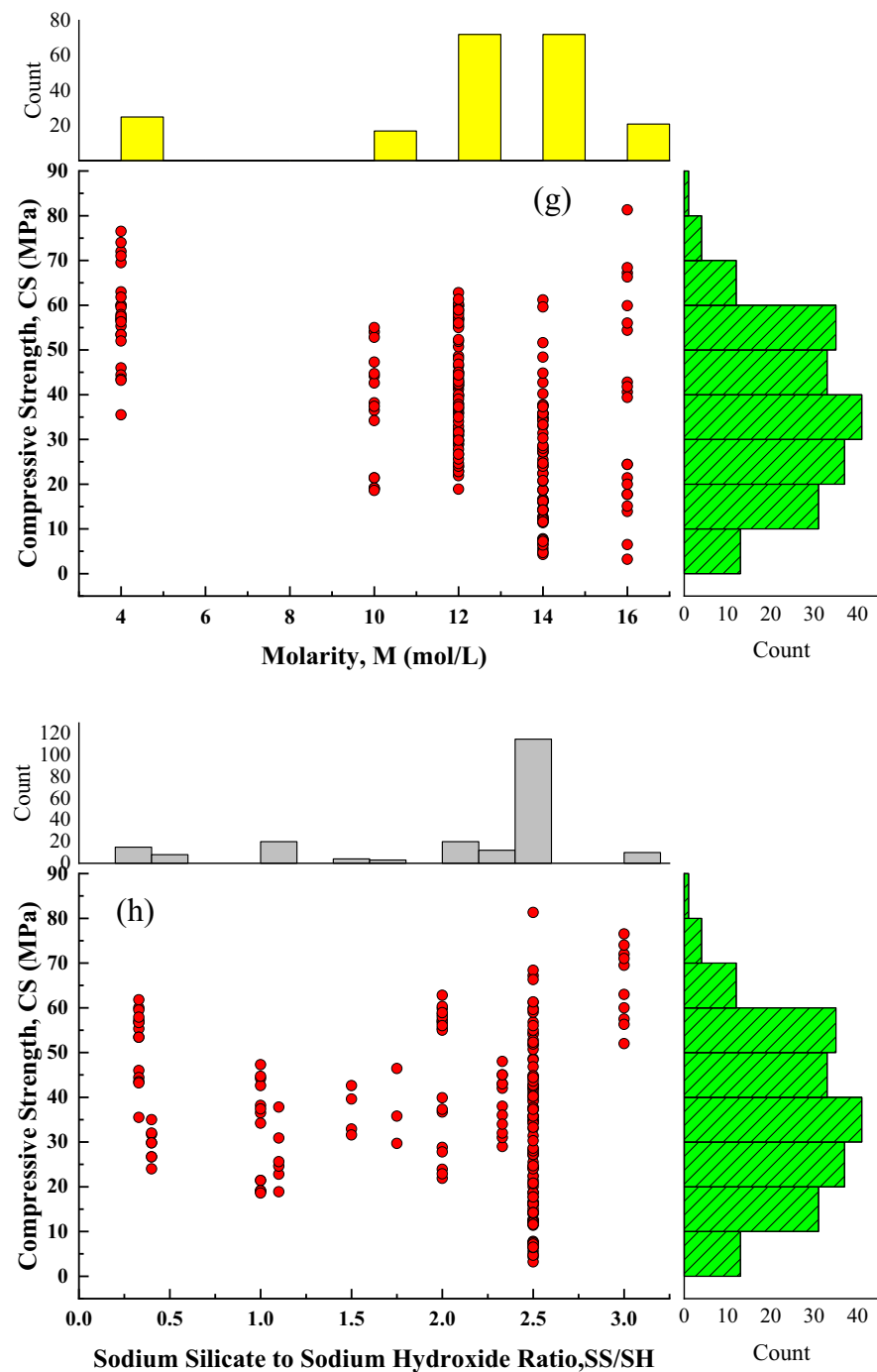
Fig. 2 continued



In this study, according to the collected datasets, the amount of SH in a 1m³ of GPC mixture incorporated nS was in the range between 18.1 and 159.7 kg/m³, with an average of 71.3 kg/m³ and a standard deviation of 33.9 kg/m³. Also, the range of SS was found in between 40.8 and 187.5 kg/m³, with an average of 134.4 kg/m³ and the standard deviations of 35.6 kg/m³. Other stats information like variance, skewness and kurtosis were 1268, -1.42 and 1.55, respectively. Moreover, the range of SS/SH was

found between 0.33 and 3, with an average of 2.05 and standard deviations of 0.76, and the other statistical criteria were found to be 0.59, -1.2 and 0.22 for the variance, skewness and kurtosis, respectively. On the other hand, the molarity of sodium hydroxide was in the range of 4 to 16 M, with an average of 11.9 M and standard deviations of 3.3 M. Also, it was found that the variance of the reviewed datasets was 11.1, the skewness was -1.4, and kurtosis was 1.3.

Fig. 2 continued

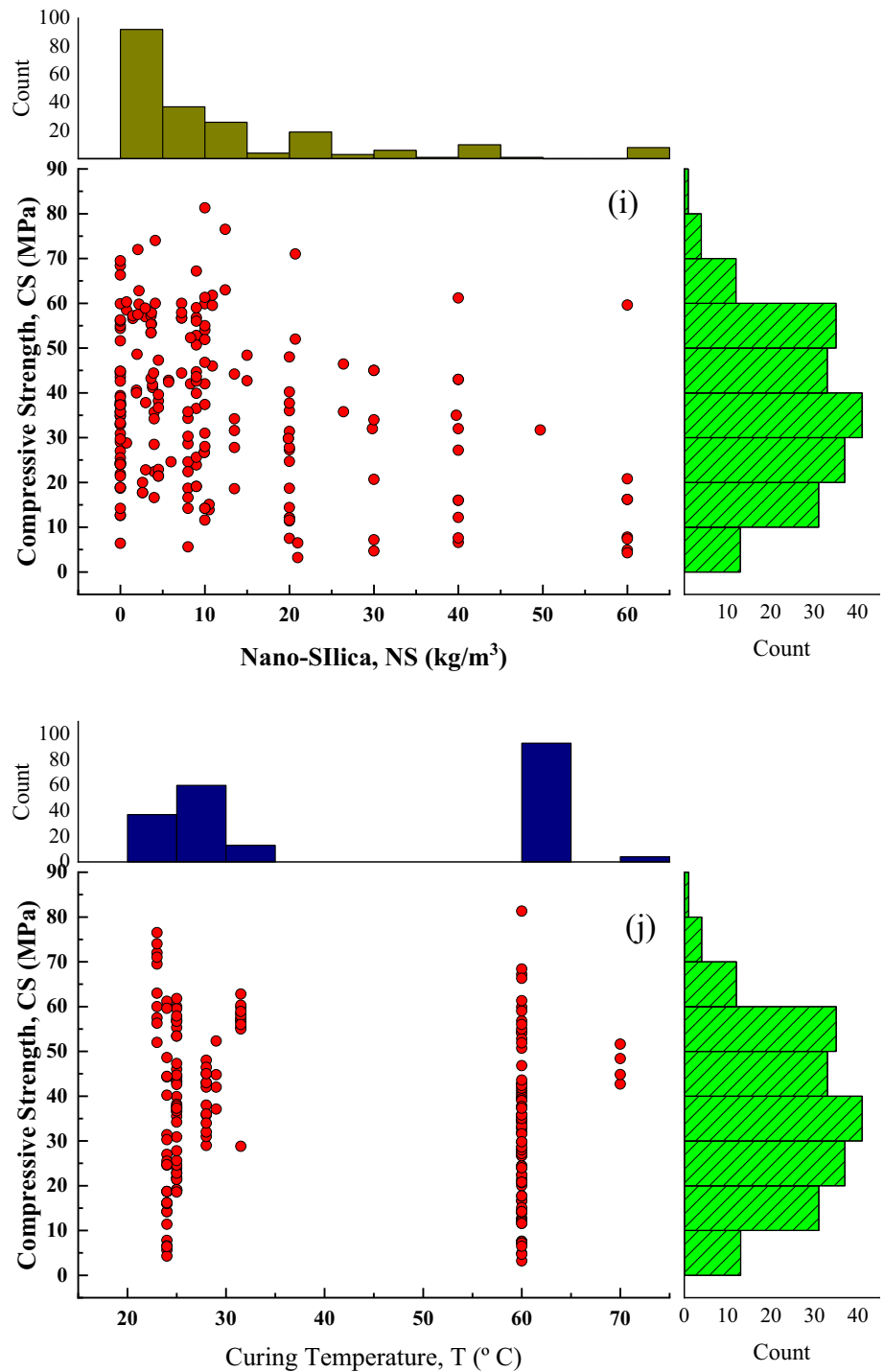


Regarding the values of nS content, it was found that the range of nS was used to improve GPC composites in the range between 0 and 60 kg/m³, with an average of 11.6 kg/m³ and the standard deviations of 14.5 kg/m³.

GPC specimens modified with nS were cured in the temperature ranges between 23 and 70 °C, with an average of 42.05 °C and the standard deviations of 17.4 °C. Also, other statistical assessment tolls like variance, skewness and kurtosis were 303.9, 0.11 and - 1.92, respectively.

The age of GPC specimens incorporated nS was ranged from 0.5 to 180 days, with an average of 28 days and standard deviations of 31.8 days. Similarly, the published datasets' variance, skewness and kurtosis were 1012.8, 2.36 and 6.96, respectively. Finally, as shown in Table 1, the range of the CS for the gathered datasets was in the range between 3.2 and 81.3 MPa, with an average of 36.2 MPa and standard deviations of 17.52 MPa. At the

Fig. 2 continued



same time, other statistical criteria like variance, skewness and kurtosis were 307, 0.15 and -0.75 , respectively.

5 Modeling

According the correlation matrix (Fig. 3), there is a poor correlation between independent variables and dependent variable, the correlations of l/b , B, FA, CA, SH, SS, M, SS/

SH, NS, T and A and with CS are -0.52 , 0.39 , 0.24 , -0.25 , -0.08 , -0.09 , -0.49 , -0.08 , -0.31 , -0.17 and 0.59 , respectively. Therefore, different multivariable models are advanced in the next section to develop an analytical model to predict the CS of GPC modified with NS.

The correlation between dependent and independent variables determines a direct relationship between the mixture proportion of the GPC and compressive strength.

Fig. 2 continued

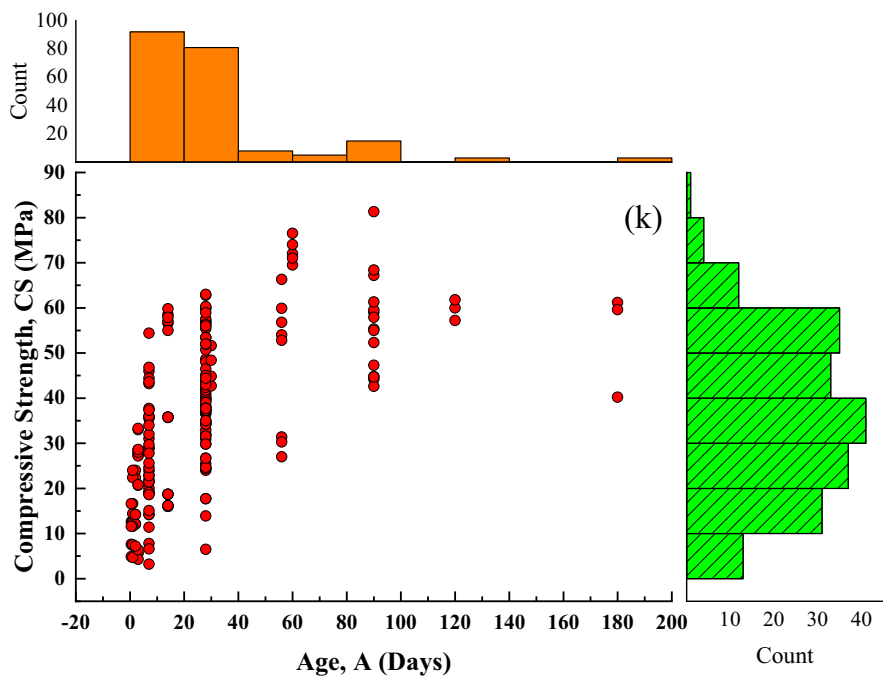


Table 2 A summary of the statistical analysis of the model’s input parameters

Model parameters	No. of data	Average	Median	St.div	Min	Max	Variance	Skewness	Kurtosis
l/b	207	0.49	0.5	0.1	0.4	0.6	0.0	0.66	− 0.25
B (kg/m ³)	207	417.22	400	51.9	300	500	2689.5	0.11	− 0.81
FA (kg/m ³)	207	680.96	650	135.3	490	990	18,294.6	0.63	− 0.10
CA (kg/m ³)	207	1113.85	1170	183.3	810	1470	33,580.8	− 0.20	− 0.72
SH (kg/m ³)	207	71.36	60	33.9	18.17	159.75	1150.6	1.10	0.49
SS (kg/m ³)	207	134.43	150	35.6	40.8	187.5	1268.2	− 1.43	1.56
M	207	11.97	12	3.3	4	16	11.1	− 1.43	1.31
SS/SH	207	2.06	2.5	0.8	0.33	3	0.6	− 1.26	0.22
NS (kg/m ³)	207	11.65	8	14.6	0	60	211.8	1.85	3.09
T (°C)	207	42.06	31.5	17.4	23	70	304.0	0.12	− 1.93
A (days)	207	28.30	28	31.8	0.5	180	1012.9	2.37	6.96
CS (MPa)	207	36.18	35.8	17.5	3.2	81.3	307.0	0.15	− 0.75

The datasets were divided into two categories at random: training and testing datasets [26]. The training dataset is used in the model development, and the testing dataset is used to check the developed model against unobserved data during training. The forecasts of various models were compared employing these criteria: (1) The model’s validity should be established scientifically; (2) between estimated and tested data, it should have a lower percentage of error; and (3) the RMSE and SI values of the suggested equations should be low, while R value should be high.

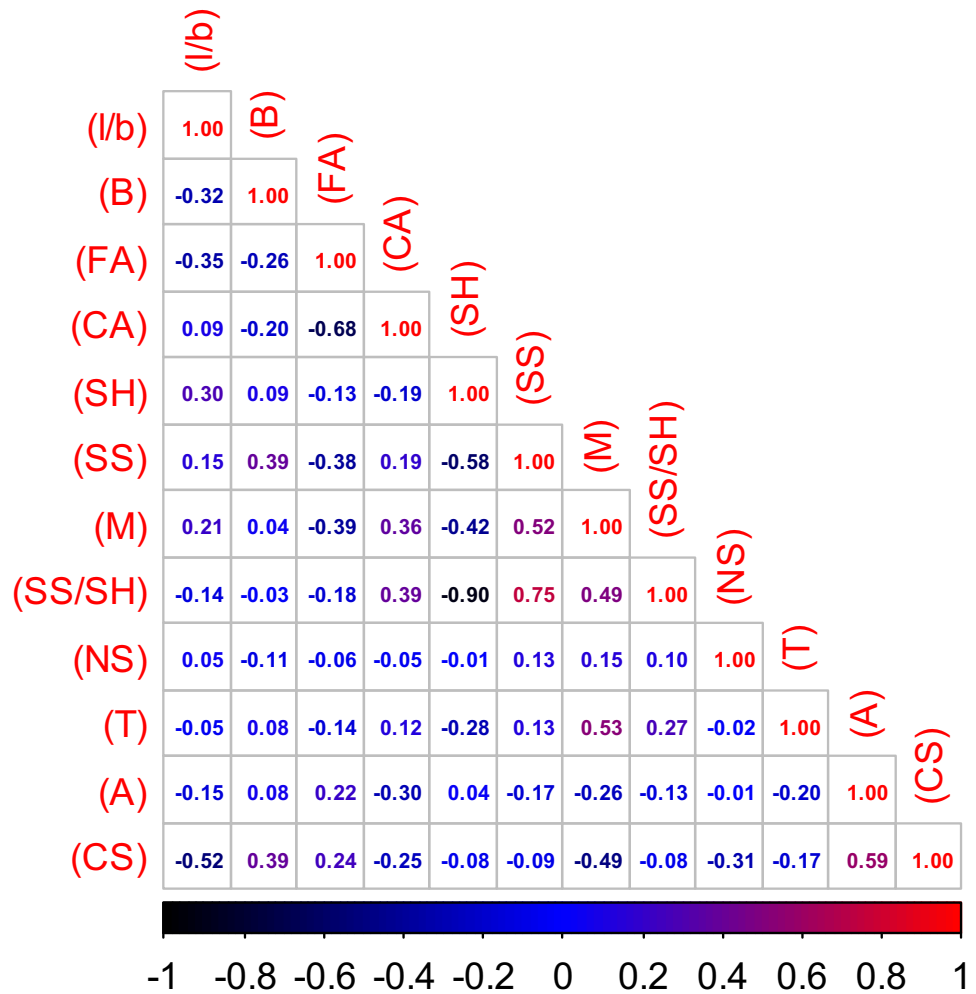
5.1 Linear regression model (LR)

Scholars adopted LR as one of the standard methodologies to estimate and forecast the CS of concrete composites [46]. As seen in Eq. (1), this model has a broad form [47].

$$CS = \beta_1 + \beta_2(x1) \tag{1}$$

where CS, x1, β_1 and β_2 represents the compressive strength, one of the variable input parameters and model parameters, respectively. This equation contains just one variable of input data, so to have more practical and reliable investigations, Eq. (2) is suggested, which contains a

Fig. 3 Correlation matrix for input variables and target



wide range of input variable data parameters that can cover all of the geopolymer concrete mixture proportions and curing conditions, as well as curing ages.

$$\begin{aligned}
 CS = & \beta_1 + \beta_2 \left(\frac{l}{b}\right) + \beta_3(b) + \beta_4(FA) + \beta_5(CA) + \beta_6(SH) \\
 & + \beta_7(SS) + \beta_8(M) + \beta_9\left(\frac{SS}{SH}\right) + \beta_{10}(NS) + \beta_{11}(T) \\
 & + \beta_{12}(A)
 \end{aligned}
 \tag{2}$$

Table 3 Optimal parameters for MEP model

Parameters	Value
Subpopulation no.	20
Subpopulation size	120
Code length	300
Crossover probability	1
Mutation probability	0.01
Operator	+, -, *, /
Tournament size	2
Function probability	0.5
Variable probability	0.5
Generations	1000

As mentioned earlier, all these main variables in Eq. (2) were described except that the $\beta_1, \beta_2, \beta_3, \dots$ and β_{12} are the model parameters. Equation (2) is a one-of-a-kind equation because it incorporates a large number of independent variables to generate GPC that may be extremely useful in the construction industry. On the other hand, because all variables can be adjusted linearly, the proposed Eq. (2) can be considered an extension of Eq. (1).

5.2 Multi-Expression Programing model (MEP)

Holland was the first to suggest a genetic algorithm (GA), which was motivated by evolution theory, comparable to the genetic programming (GA) developed by Cramer [48].

Several linear GP modifications have already been proposed to address some of the issues (such as bloat) that tree representations of GP produce. A few examples are cartesian genetic programming, grammatical evolution (GE), linear GP and gene expression programming [49]. In MEP individuals, multiple solutions are stored on a different chromosome. In most cases, the most acceptable choice is

5.3 Full quadratic model model (FQ)

The FQ model was made using the full quadratic formula, which is shown in Eq. (3). This formula is a relationship between compressive strength and the first and second degree of each independent variable and the interaction between independent variables [51].

$$\begin{aligned}
 CS = & \beta_1 \left(\frac{l}{b}\right) + \beta_2(B) + \beta_3(FA) + \beta_4(CA) + \beta_5(SH) + \beta_6(SS) + \beta_7(M) + \beta_8 \left(\frac{SS}{SH}\right) + \beta_9(NS) \\
 & + \beta_{10}(T) + \beta_{11}(A) + \beta_{12} \left(\frac{l}{b}\right)^2 + \beta_{13}(B)^2 + \beta_{14}(FA)^2 + \beta_{15}(CA)^2 + \beta_{16}(SH)^2 \\
 & + \beta_{17}(SS)^2 + \beta_{18}(M)^2 + \beta_{19} \left(\frac{SS}{SH}\right)^2 + \beta_{20}(NS)^2 + \beta_{21}(T)^2 + \beta_{22}(A)^2 \\
 & + \beta_{23} \left(\frac{l}{b}\right)(B) + \beta_{24} \left(\frac{l}{b}\right)(FA) + \beta_{25} \left(\frac{l}{b}\right)(CA) + \beta_{26} \left(\frac{l}{b}\right)(SH) + \beta_{27} \left(\frac{l}{b}\right)(SS) \\
 & + \beta_{28} \left(\frac{l}{b}\right)(M) + \beta_{29} \left(\frac{l}{b}\right) \left(\frac{SS}{SH}\right) + \beta_{30} \left(\frac{l}{b}\right)(NS) + \beta_{31} \left(\frac{l}{b}\right)(T) + \beta_{32} \left(\frac{l}{b}\right)(A) \\
 & + \beta_{33}(B)(FA) + \beta_{34}(B)(CA) + \beta_{35}(B)(SH) + \beta_{36}(B)(SS) + \beta_{37}(B)(M) \\
 & + \beta_{38}(B) \left(\frac{SS}{SH}\right) + \beta_{39}(B)(NS) + \beta_{40}(B)(T) + \beta_{41}(B)(A) + \beta_{42}(FA)(CA) \\
 & + \beta_{43}(FA)(SH) + \beta_{44}(FA)(SS) + \beta_{45}(FA)(M) + \beta_{46}(FA) \left(\frac{SS}{SH}\right) + \beta_{47}(FA)(NS) \\
 & + \beta_{48}(FA)(T) + \beta_{49}(FA)(A) + \beta_{50}(CA)(SH) + \beta_{51}(CA)(SS) + \beta_{52}(CA)(M) \\
 & + \beta_{53}(CA) \left(\frac{SS}{SH}\right) + \beta_{54}(CA)(NS) + \beta_{55}(CA)(T) + \beta_{56}(CA)(A) + \beta_{57}(SH)(SS) \\
 & + \beta_{58}(SH)(M) + \beta_{59}(SH) \left(\frac{SS}{SH}\right) + \beta_{60}(SH)(NS) + \beta_{61}(SH)(T) + \beta_{62}(SH)(A) \\
 & + \beta_{63}(SS)(M) + \beta_{64}(SS) \left(\frac{SS}{SH}\right) + \beta_{65}(SS)(NS) + \beta_{66}(SS)(T) + \beta_{67}(SS)(A) \\
 & + \beta_{68}(M) \left(\frac{SS}{SH}\right) + \beta_{69}(M)(NS) + \beta_{70}(M)(T) + \beta_{71}(M)(A) + \beta_{72} \left(\frac{SS}{SH}\right)(NS) \\
 & + \beta_{73} \left(\frac{SS}{SH}\right)(T) + \beta_{74} \left(\frac{SS}{SH}\right)(A) + \beta_{75}(NS)(T) + \beta_{76}(NS)(A) \\
 & + \beta_{77}(T)(A)
 \end{aligned} \tag{3}$$

chosen. This is characterized as strong implicit parallelism, and it is one of the MEP’s distinguishing features [50]. When compared to GE and GEP, this feature does not make MEP more complex. To establish a generalized relationship, the MEP model integrates many fitting parameters. This study used simple arithmetic operators to produce simple expressions, and the fitting parameters were determined using a trial-and-error technique, as depicted in Table 3.

where all these main variables in Eq. (3) were described except that the $\beta_1, \beta_2, \beta_3, \dots$ and β_{77} are the model parameters.

5.4 Artificial neural network (ANN)

Multilayer perceptron is a feed-forward artificial neural network (ANN) model composed of neurons with heavily weighted interconnections, where signals always move in

the output layer direction. ANN is a powerful piece of simulation software that was developed for data analysis and computation. It processes and analyzes data in a manner that is analogous to that of the human brain. This tool for machine learning sees extensive application in the field of construction engineering, namely for predicting the outcomes of a wide range of numerical issues [52].

The input, hidden and output layers make up ANN. The input layer captures variables from the outer environment for use in model training and testing. The hidden layer is responsible for connecting the input and output layers and comprises activation functions such as hyperbolic tangent sigmoid, log-sigmoid and exponential linear units. The output layer represents the result of the model. Each layer is composed of multiple parallel neurons (nodes) that are components of information processing and are weighted and connected to the next layer of nodes [53].

No standard method exists for building network architecture. Consequently, the number of hidden layers and neurons is established via trial and error. One of the key objectives of the network training procedure is to discover the optimal number of iterations (epochs) that yield the lowest RMSE and closest R-value to one. The designed ANN was trained and tested for different hidden layers to find the best network structure based on how well the predicted CS of GPC and the actual CS of the collected data fit together. To train the developed ANN, the acquired dataset (a total of 205 data) was separated into two sections. Approximately 70% of the obtained data was utilized for training the network as trained data. The dataset was tested using 30% of the total data [54]. The ANN structure with one hidden layer, 6 neurons and a hyperbolic tangent transfer function was found to be the best-trained network with the highest R and the lowest RMSE. Equations (4), (5) and (6) reveal the ANN model’s general equations [55].

From linear node 0:

$$CS = \text{Threshold} + \left(\frac{\text{Node1}}{1 + e^{-B1}}\right) + \left(\frac{\text{Node2}}{1 + e^{-B2}}\right) + \dots + \left(\frac{\text{Noden}}{1 + e^{-Bn}}\right) \tag{4}$$

From sigmoid node 1:

$$B1 = \text{Threshold} + \Sigma(\text{Attribute} * \text{Variable}) \tag{5}$$

From sigmoid node 2:

$$B2 = \text{Threshold} + \Sigma(\text{Attribute} * \text{Variable}) \tag{6}$$

5.5 M5P-tree model (M5P)

The M5 algorithm was utilized to construct and expand the M5P algorithm. The M5P algorithm, unlike other decision

tree algorithms, mixes a typical linear regression model with the nodes of a decision tree. It is possible to store linear models that forecast the studied object at the tree nodes. The M5P algorithm is, therefore, a model of segmented linear functions that transforms classification into functional optimization. M5P is an algorithm for the numerical prediction that has broad application potential and many advantages, such as high efficiency and resilience. The M5P supports binary, integer, nominal and missing attribute values [56].

By using this learner approach, the linear regression functions are inserted at the terminal nodes. A multivariate linear regression model is assigned to the subspace by classifying all datasets into various subspaces. The M5P-tree technique is capable of handling jobs with a high number of dimensions and acts on continuous class issues rather than discrete segments. It provides the produced information of each linear model component used to estimate the nonlinear correlation between the datasets. The information regarding the M5-tree model’s division criteria is obtained by calculating error at each node. Errors are analyzed using the standard deviation of the class entering that node at each node. At each node, the attribute that maximizes the decrease of estimated error is used to evaluate every task that the node does. This partition of the M5P tree will result in the generation of a huge treelike structure, which will lead to overfitting. The massive tree is pruned in the subsequent stage, and linear regression functions restore the cut subtrees [45]. The M5P-tree model has the same general equation form as the linear regression equation, as seen in Eq. (7).

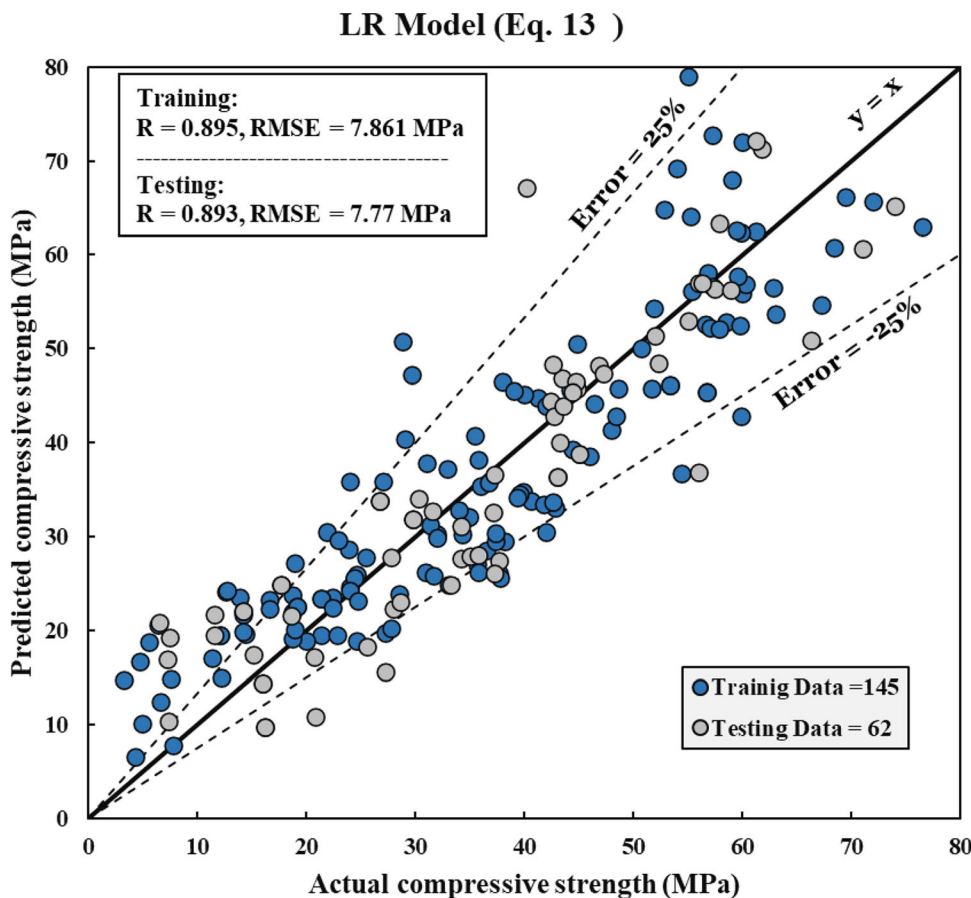
$$CS = \beta_1 + \beta_2 \left(\frac{l}{b}\right) + \beta_3(b) + \beta_4(FA) + \beta_5(CA) + \beta_6(SH) + \beta_7(SS) + \beta_8(M) + \beta_9 \left(\frac{SS}{SH}\right) + \beta_{10}(NS) + \beta_{11}(T) + \beta_{12}(A) \tag{7}$$

where the descriptions of all of the variables in this Eq. (7) were provided earlier.

6 Model efficiencies

To rate and evaluate the accuracy of the presented models, several performance statistics techniques including R, RMSE, SI and OBJ, using the following equations were utilized:

Fig. 4 Comparison between tested and predicted CS of GPC mixtures modified with NS using LR model for training and testing datasets



$$R^2 = \left(\frac{\sum_{p=1}^n (y_p - y)(x_p - x')}{\sqrt{[\sum_{p=1}^n (y_p - y')^2][\sum_{p=1}^n (x_p - x')^2]}} \right)^2 \tag{8}$$

$$R = \sqrt[3]{R} \tag{9}$$

$$RMSE = \sqrt{\frac{\sum_{p=1}^n (x_p - y_p)^2}{n}} \tag{10}$$

$$SI = \frac{RMSE}{y'} \tag{11}$$

$$OBJ = \left(\frac{n_{tr}}{n_{all}} * \frac{RMSE_{tr} + MAE_{tr}}{R^2_{tr} + 1} \right) + \left(\frac{n_{tst}}{n_{all}} * \frac{RMSE_{tst} + MAE_{tst}}{R^2_{tst} + 1} \right) \tag{12}$$

where x_p and y_p are estimated and tested CS values, y' and x' are averages of experimentally tested and the estimated values from the models, respectively. tr and tst are referred to like the training and testing datasets, respectively, and n is the number of datasets. Zero is the optimal value for all other evaluation parameters except for the R value. However, one is the highest benefit for R. When it comes to the SI parameter, a model has bad performance when it is >

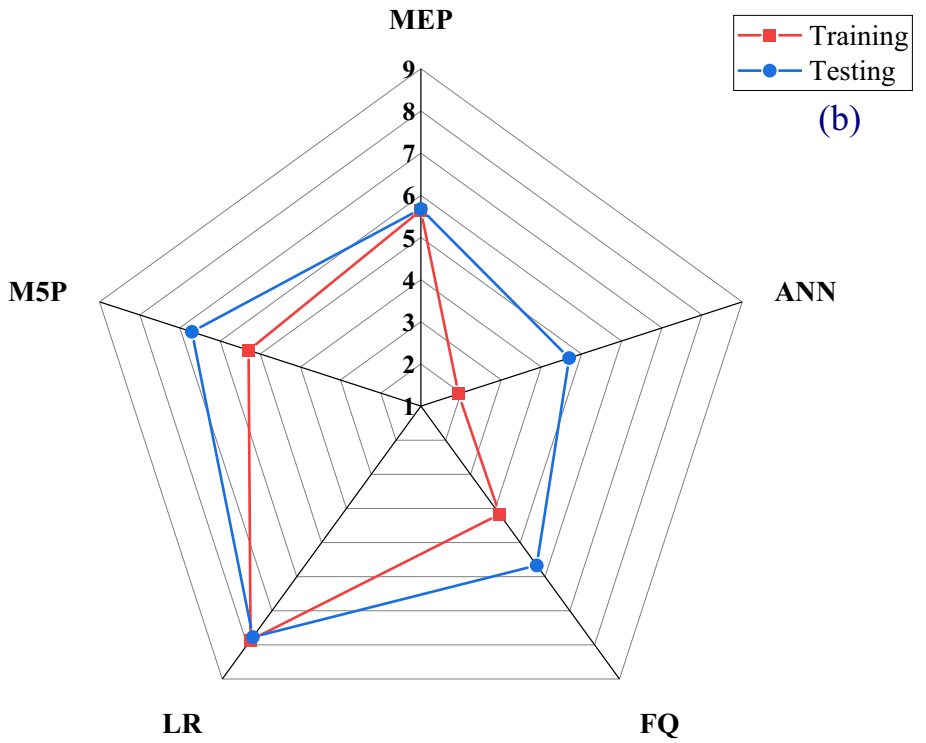
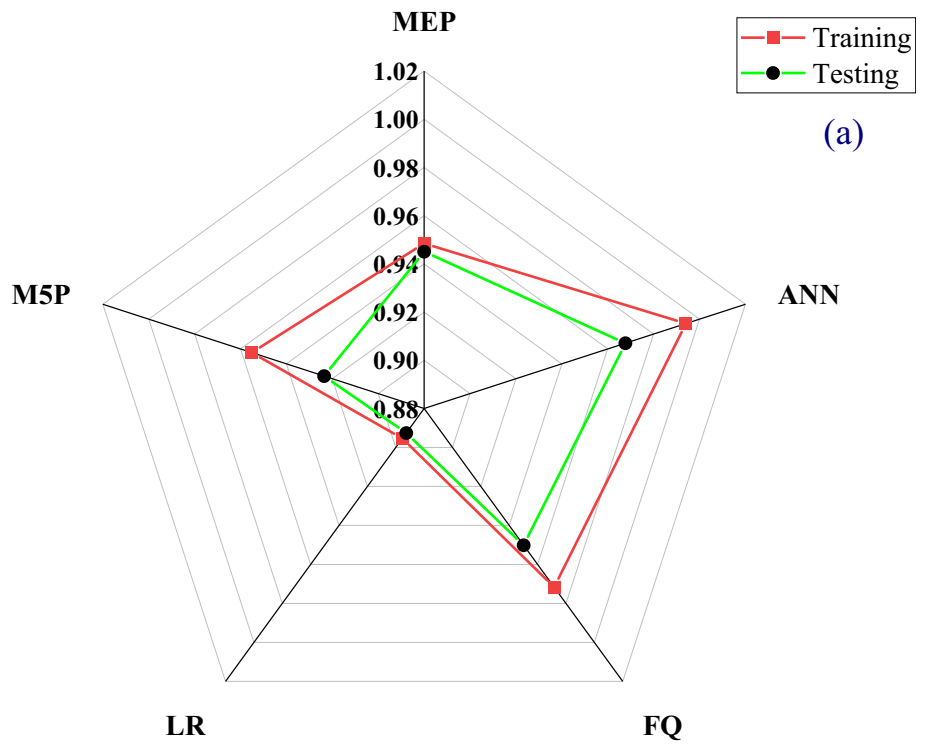
0.3, acceptable performance when it is 0.2 SI 0.3, excellent performance when it is 0.1 SI 0.2 and great performance when it is 0.1 SI 0.1 [57]. Furthermore, the OBJ parameter was employed as a performance measurement parameter in Eq. (12) to measure the efficiency of the suggested models.

7 Results and analysis

7.1 LR model

This model’s output demonstrated that the l/b and SS/SH parameters had a bigger influence on the CS of GPC than any other factors. This result was supported by experimental efforts published in the scientific literature [58]. This model’s output is Eq. (13) weighted by each model parameter. The weighting of each parameter on the CS of GPC mixtures, including NS was determined by optimizing the sum of error squares and the least square approach, which were implemented in an Excel program using Solver to calculate the optimum answer for the equation in one cell called the objective cell. This worksheet object cell

Fig. 5 Radar plot for comparison between developed models based on: **a**: correlation coefficient and **b**: root-mean-square error



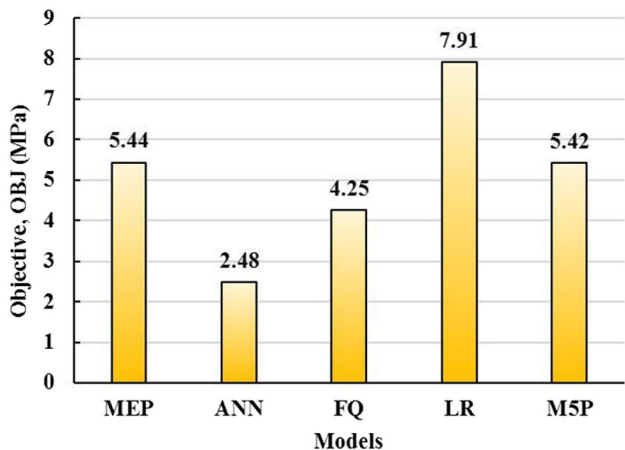


Fig. 6 Comparing the OBJ performance parameter of different developed models

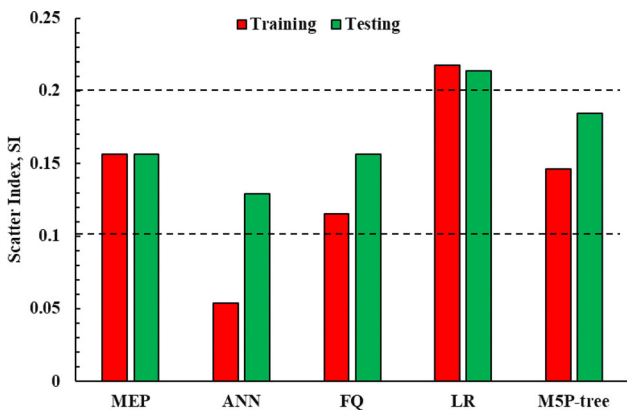
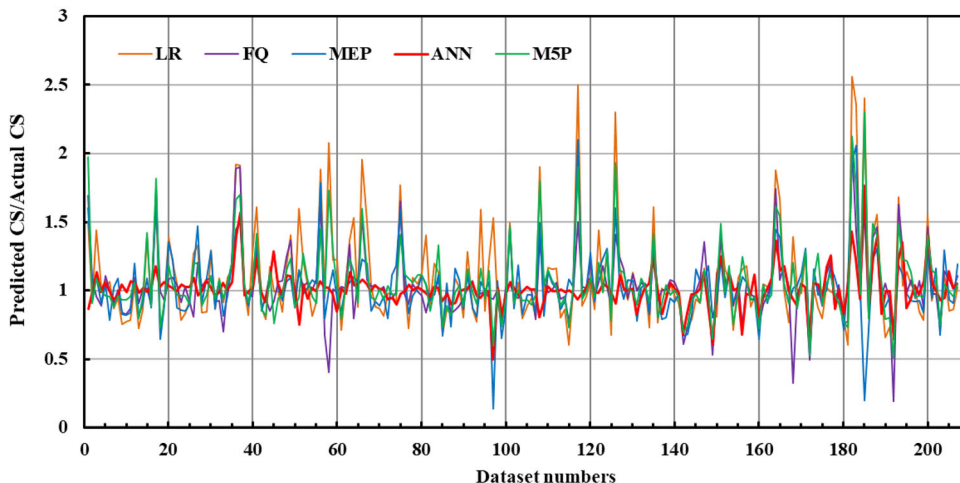


Fig. 7 Comparing the SI performance parameter of different developed models

was bound by the values of the cells containing other equations [46].

Fig. 8 CS of GPC mixes residual error diagram utilizing entire datasets for all models



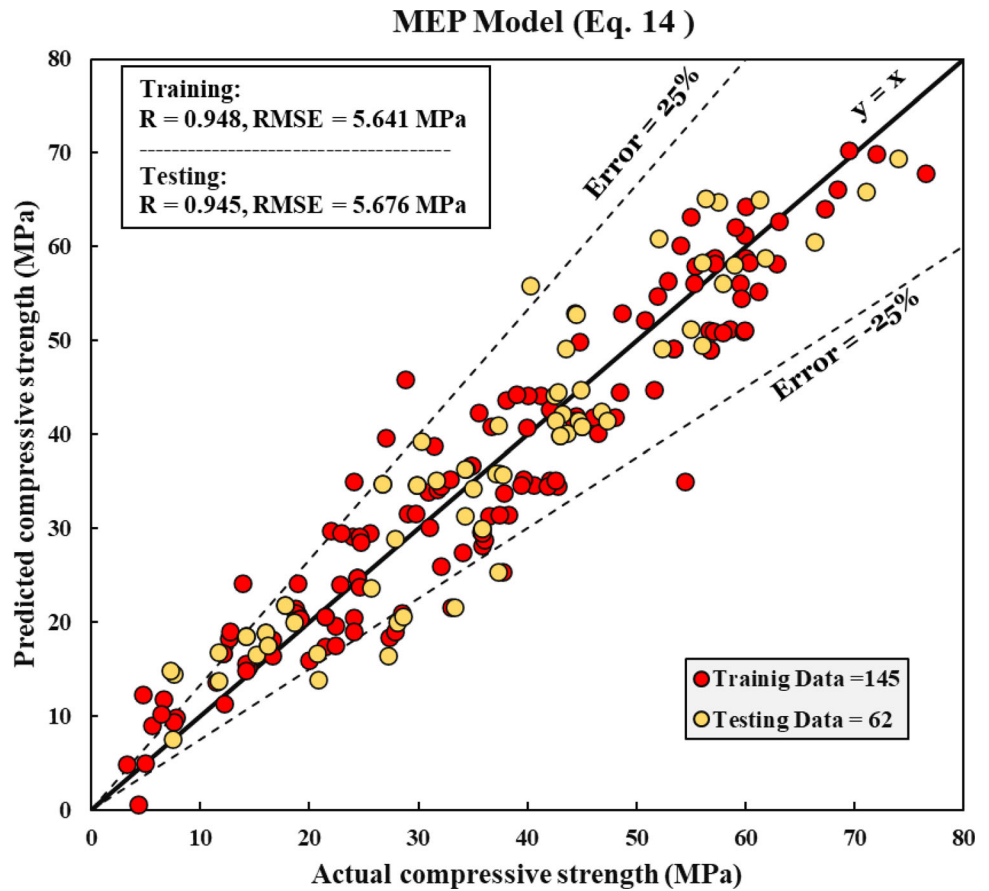
$$\begin{aligned}
 CS = & 115.2 - 84.5 \left(\frac{l}{b}\right) + 0.0559(B) - 0.0165(FA) \\
 & + 0.01600(CA) - 0.3870(SH) \\
 & + 0.1589(SS) - 2.839(M) - 18.50 \left(\frac{SS}{SH}\right) \\
 & - 0.1992(NS) + 0.1197(T) \\
 & + 0.2892(A)
 \end{aligned}
 \tag{13}$$

Figure 4 depicts the relationship between estimated and real CS of GPC mixtures incorporated nS for training and testing datasets. Moreover, this model was evaluated by some statistical assessment tools, and it was observed that the R (Fig. 5a) and RMSE (Fig. 5b) for the training datasets were equal to 0.895 and 7.861 MPa, respectively. Moreover, as illustrated in Figs. 6 and 7, the other statistical criteria like OBJ and SI were 7.91 MPa and 0.217, respectively. Finally, utilizing the training and testing datasets, normalized predicted CS/actual CS versus the number of datasets for all the models is shown in Fig. 8. The application of this model is straightforward, the only limitation is the lower capability to predict the CS with a higher percentage of errors compared to other models.

7.2 MEP model

Figure 9 displays the correlations between the actual and predicted CS of GPC mixtures modified with NS for the training and testing datasets. The graph displayed error lines ranging from ± 25% for training and testing datasets with R and RMSE values of 0.948 and 5.64 MPa for training datasets and 0.945 and 5.68 MPa for testing datasets. The MEP modeling result was decoded to get Eq. (14) [59], which can be utilized to estimate the CS of GPC modified with NS.

Fig. 9 Comparison between actual and predicted CS of GPC mixtures modified with NS using MEP model for training and testing datasets



$$CS = \gamma_1 - \gamma_2 - \frac{\gamma_3}{\gamma_4} \tag{14}$$

$$\gamma_1 = \frac{b - \left(\frac{b \cdot h}{e + \frac{k}{g}} + 2 \times \left(\frac{f}{\left(\frac{i}{g} + k \right) * (4g +)} \right) + 4g \right)}{g + \frac{c}{f + b}} \tag{14 - 1}$$

$$\gamma_2 = \left(\frac{4g - j}{\frac{k}{2g} - 4g + e} + \frac{i}{k + \frac{j}{g} + k} \right) + \frac{\left(\frac{i}{g} + k \right) * (4g)}{e + \frac{k}{2g} + \frac{j}{g} + k + \frac{d}{b}} - h \tag{14 - 2}$$

$$\gamma_3 = \frac{e + \frac{k}{2g} + \frac{\frac{\frac{l}{g} + k + 4g - j}{\frac{l}{g} + k + 4g - j - \left(\frac{l}{g} + k + \frac{d}{b} \right)}}{\frac{l}{g} + k + 4g - j - \left(\frac{l}{g} + k + \frac{d}{b} \right)}}{4g} \tag{14 - 3}$$

$$\gamma_4 = \left(\frac{4g - j}{\frac{k}{2g} - (4g) + e} \right) * \left(\frac{c}{g * \left(\frac{k}{2g} - (4g) \right)} \right) + a \tag{14 - 4}$$

where $a = 1/b$, $e = SH$, $i = NS$, $b = B$, $f = SS$, $j = T$, $c = FA$, $g = M$, $k = A$, $d = CA$, $h = SS/SH$.

Like the LR model, this model was also assessed by some statistical criteria. The OBJ and SI were equal to 5.44 MPa and 0.156, respectively, as illustrated in Figs. 6 and 7. Lastly, utilizing the training and testing datasets, normalized predicted CS/actual CS versus the number of datasets for all the models is shown in Fig. 8. While this model has good efficiency to predict the CS of GPC modified with NS, its equations are somewhat lengthy and need more calculation procedures.

7.3 FQ model

Equation (15) is the output of the FQ model with various variable parameters. The most influential independent factors on the CS of the geopolymer concrete mixtures altered with NS in the FQ model were binder content, the SS amount, the age of the specimens and the curing temperatures, which are consistent with previous experimental results [60].

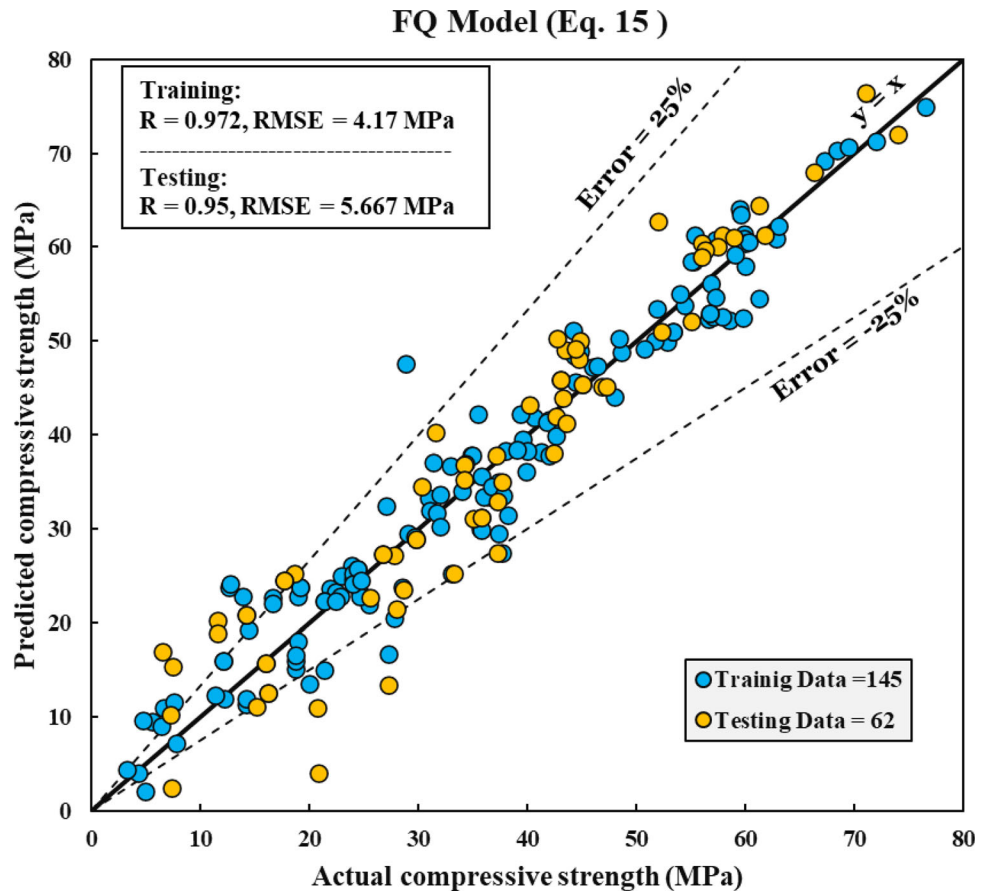
Using training and testing datasets, the expected and measured CS correlations for the GPC mixtures adjusted with NS are illustrated in Fig. 10. In addition, similar to past models, this model was evaluated using testing data to establish its applicability to variables not included in the

model data (training data). The results show that by plugging the independent variables into the constructed equation, this model can accurately predict the CS of GPC. This model was assessed using certain statistical tools, and the values of R and RMSE were found to be 0.972 and 4.17 MPa, respectively, for the training datasets and 0.95 and 5.667 MPa, respectively, for the testing datasets. In addition, as shown in Figs. 6 and 7, the values of other statistical assessment methods such as OBJ and SI were

found to be 4.25 MPa and 0.115, respectively. Finally, the normalized predicted CS/actual CS versus the number of datasets for all models was examined using the training and testing datasets, as shown in Fig. 8. The only limitation of the current model is its lengthy equation, which can be easily overcome by training the equation in any software such as excel program.

$$\begin{aligned}
 CS = & -0.0004\left(\frac{l}{b}\right) + 1.483(B) - 1.2278(FA) + 0.2606(CA) + 0.0096(SH) + 0.3215(SS) \\
 & - 0.0088(M) - 0.0117\left(\frac{SS}{SH}\right) + 0.0154(NS) + 0.0238(T) \\
 & - 0.0181(A) - 0.0001\left(\frac{l}{b}\right)^2 - 0.0009(B)^2 + 0.0004(FA)^2 - 0.0001(CA)^2 \\
 & - 0.00005(SH)^2 - 0.00004(SS)^2 - 0.0118(M)^2 - 0.1756\left(\frac{SS}{SH}\right)^2 \\
 & - 0.0018(NS)^2 - 0.0389(T)^2 - 0.0026(A)^2 - 1.6016\left(\frac{l}{b}\right)(B) + 1.0703\left(\frac{l}{b}\right)(FA) \\
 & - 0.0002\left(\frac{l}{b}\right)(CA) - 0.0936\left(\frac{l}{b}\right)(SH) - 0.0021\left(\frac{l}{b}\right)(SS) - 0.0085\left(\frac{l}{b}\right)(M) \\
 & - 0.0067\left(\frac{l}{b}\right)\left(\frac{SS}{SH}\right) + 0.0048\left(\frac{l}{b}\right)(NS) - 0.0011\left(\frac{l}{b}\right)(T) + 0.0027\left(\frac{l}{b}\right)(A) \\
 & + 0.0001(B)(FA) + 0.0001(B)(CA) - 0.00002(B)(SH) + 0.00001(B)(SS) \\
 & + 0.00003(B)(M) - 0.00007(B)\left(\frac{SS}{SH}\right) + 0.0019(B)(NS) - 0.00003(B)(T) \\
 & + 0.00003(B)(A) + 0.00001(FA)(CA) - 0.00017(FA)(SH) - 0.0005(FA)(SS) \\
 & + 0.0008(FA)(M) + 0.00006(FA)\left(\frac{SS}{SH}\right) + 0.0001(FA)(NS) + 0.001(FA)(T) \\
 & + 0.00006(FA)(A) + 0.000008(CA)(SH) - 0.00005(CA)(SS) - 0.0001(CA)(M) \\
 & + 0.00001(CA)\left(\frac{SS}{SH}\right) - 0.00007(CA)(NS) - 0.00009(CA)(T) + 0.0004(CA)(A) \\
 & + 0.0015(SH)(SS) - 0.0793(SH)(M) + 0.00001(SH)\left(\frac{SS}{SH}\right) \\
 & + 0.000017(SH)(NS) + 0.0107(SH)(T) + 0.00002(SH)(A) + 0.00016(SS)(M) \\
 & + 0.00006(SS)\left(\frac{SS}{SH}\right) + 0.000039(SS)(NS) + 0.0001(SS)(T) + 0.00068(SS)(A) \\
 & - 1.2328(M)\left(\frac{SS}{SH}\right) - 0.0351(M)(NS) + 0.1313(M)(T) + 0.0016(M)(A) \\
 & - 0.02468\left(\frac{SS}{SH}\right)(NS) + 0.2652\left(\frac{SS}{SH}\right)(T) - 0.02259\left(\frac{SS}{SH}\right)(A) - 0.0071(NS)(T) \\
 & + 0.0041(NS)(A) - 0.0003(T)(A)
 \end{aligned}
 \tag{15}$$

Fig. 10 Comparison between actual and predicted CS of GPC mixtures modified with NS using FQ model for training and testing datasets



7.4 ANN model

In this study, the authors applied various numbers of the hidden layer, neurons, momentum, learning rate and iteration to maximize the ANN’s performance, and it was discovered that when the ANN has one hidden layer, 6 neurons (as depicted in Fig. 11), 0.2 momentum, 0.1 learning rate and 50,000 iterations, the CS values of GPC mixtures modified with NS are most accurately predicted. The output of this proposed model is reported as shown in Eq. (16), while the results of weights and biases are shown in the matrix below.

The ANN model was equipped with the training datasets, accompanied by testing datasets to predict the CS values for the correct input parameters. The comparison between estimated and experimentally tested CS of GPC mixtures modified with NS for training and testing datasets is presented in Fig. 12. The consumed data have a ± 15% error line for the training and testing datasets, which is better than the other developed models. Furthermore, this

model has a better performance than other models in predicting the CS of the GPC based on the value of OBJ and SI illustrated in Figs. 6 and 7. Also, the value of $R = 0.994$ and $RMSE = 1.935$ MPa for the training datasets, and the R-value for the testing data was equal to 0.968, while the RMSE was equal to 4.69 MPa. Figure 8 depicts the relationship between the normalized predicted CS/actual CS and the number of datasets for all models utilizing the training and testing datasets. While the ANN-based models are very efficient to be used in the construction sector, the only significant limitation is the black-box nature of the model, in which the user can only see the outputs of the model after using different trials.

$$CS = \frac{2.016}{1 + e^{-\alpha_1}} - \frac{2.058}{1 + e^{-\alpha_2}} - \frac{8.085}{1 + e^{-\alpha_3}} + \frac{1.004}{1 + e^{-\alpha_4}} + \frac{1.558}{1 + e^{-\alpha_5}} - \frac{1.672}{1 + e^{-\alpha_6}} - 0.553 \tag{16}$$

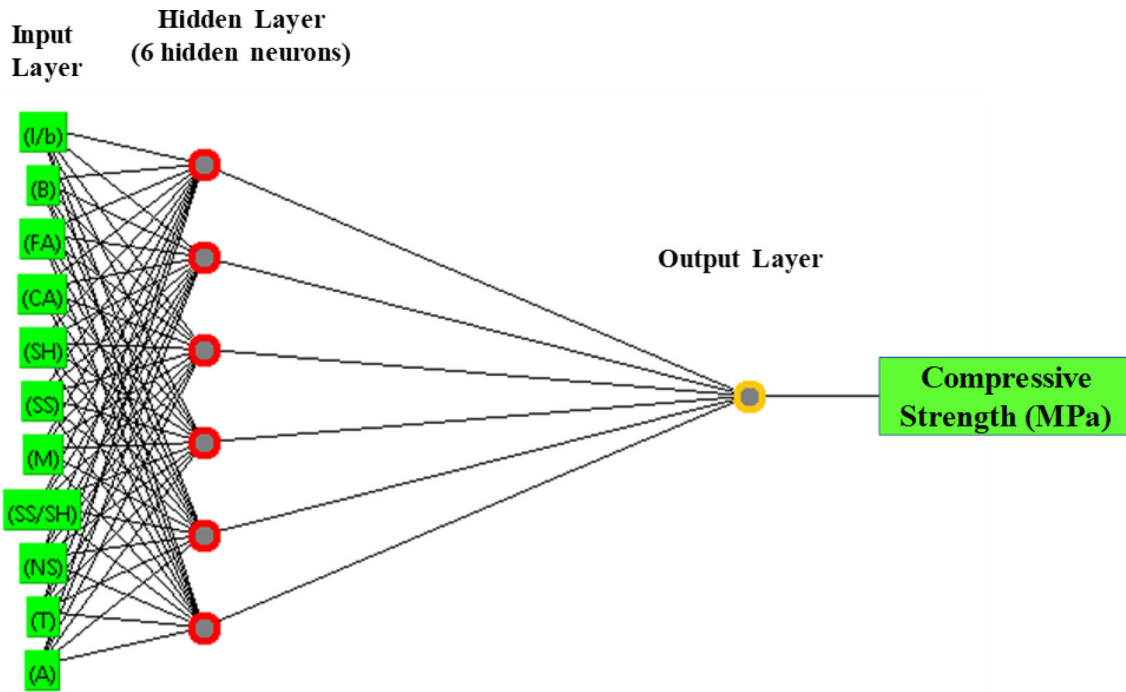


Fig. 11 Optimal network structures of the ANN model

Fig. 12 Comparison between actual and predicted CS of GPC mixtures modified with NS using ANN model for training and testing datasets

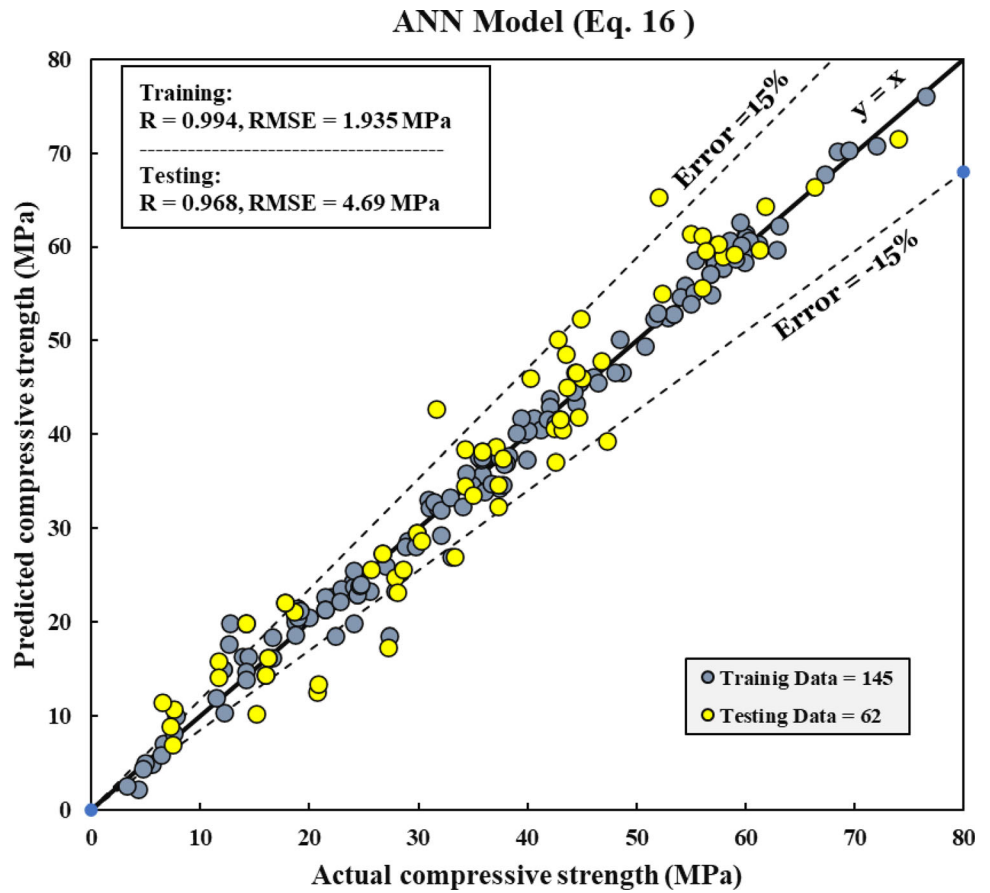


Fig. 13 Comparison between tested and predicted CS of GPC mixtures modified with NS using M5P-tree model for training and testing datasets

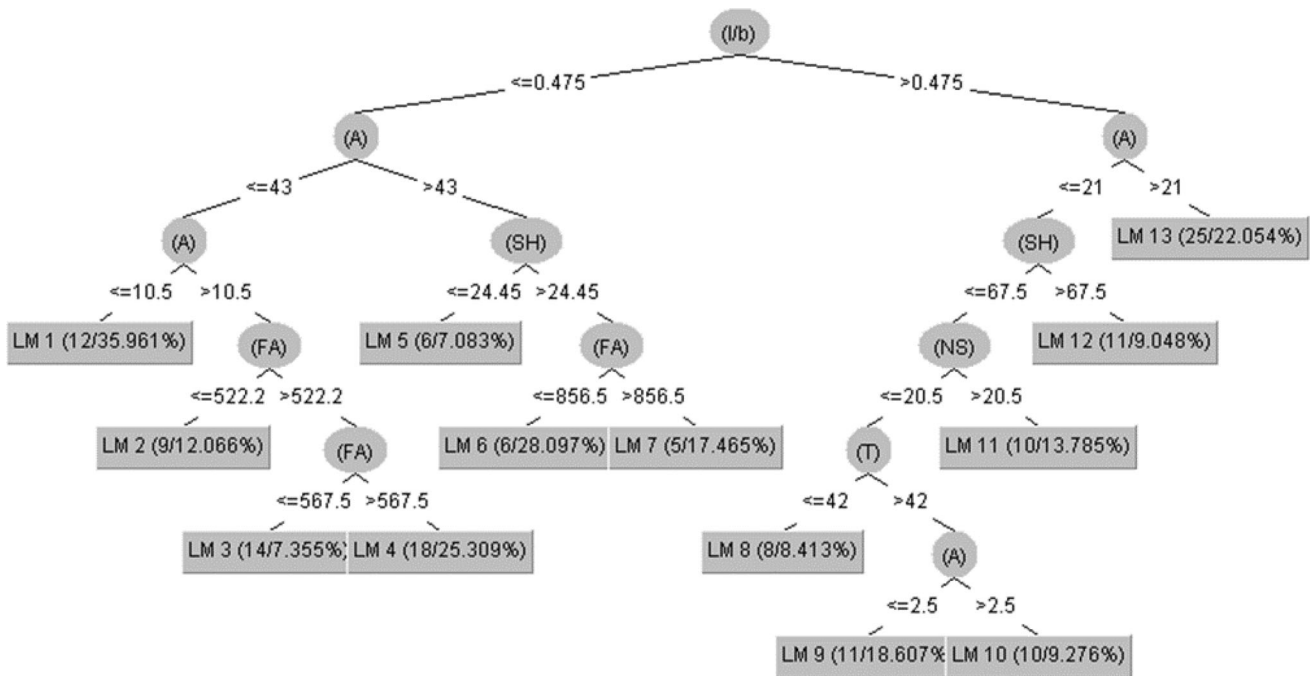
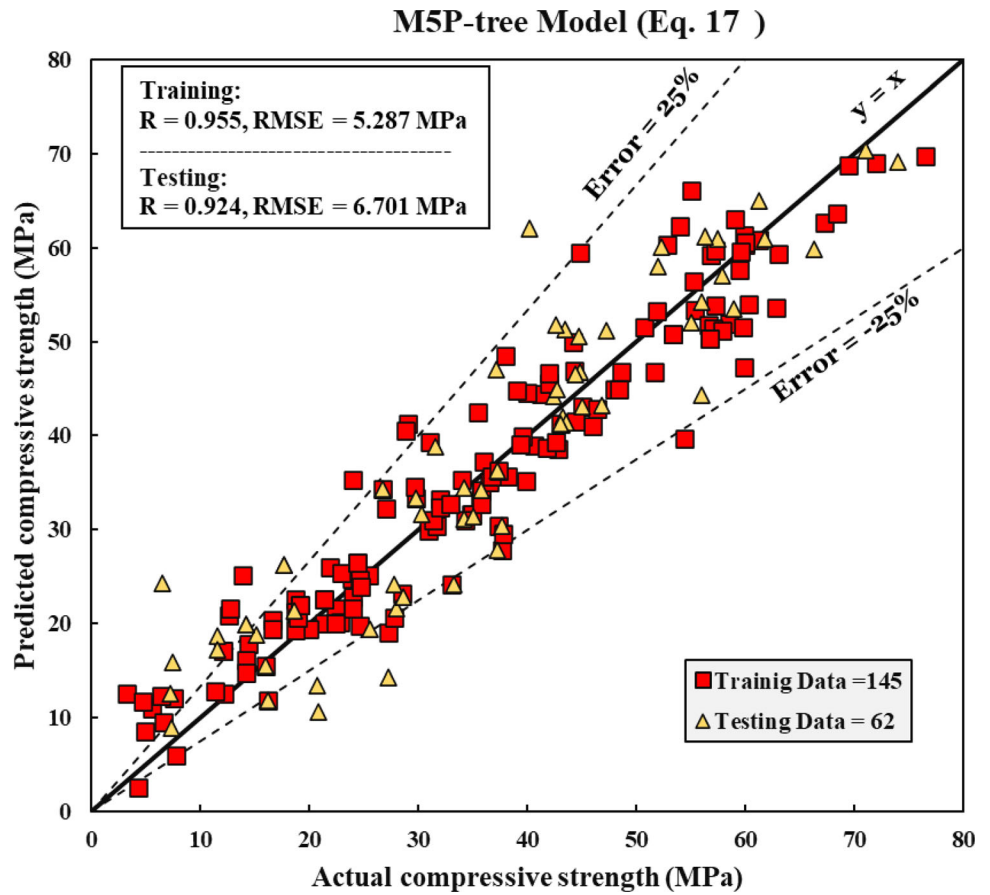


Fig. 14 M5P-tree Pruned model tree

Table 4 M5P-tree model parameters (Eq. (17))

LM	$CS = \beta_1 + \beta_2\left(\frac{l}{b}\right) + \beta_3(b) + \beta_4(FA) + \beta_5(CA) + \beta_6(SH) + \beta_7(SS) + \beta_8(M) + \beta_9\left(\frac{SS}{SH}\right) + \beta_{10}(NS) + \beta_{11}(T) + \beta_{12}(A)$										
	β_1	β_2	β_3	β_4	β_5	β_6	β_7	β_8	β_9	β_{10}	β_{11}
1	1.012	78.015	0.062	0.005	0.002	- 0.129	- 0.056	- 1.035	- 0.139	- 0.102	0.230
2	16.297	78.015	0.062	- 0.004	0.002	- 0.129	- 0.035	- 1.303	- 0.167	- 0.102	0.151
3	52.454	0.763	0.031	0.002	0.002	- 0.129	- 0.028	- 1.413	- 0.100	- 0.029	0.151
4	33.934	31.271	0.053	0.001	0.002	- 0.129	- 0.031	- 1.645	- 0.126	0.010	0.151
5	- 3.694	165.782	0.099	- 0.024	0.002	- 0.037	- 0.174	- 0.453	- 0.033	- 0.216	0.110
6	0.011	165.782	0.108	- 0.027	0.002	- 0.227	- 0.174	- 0.453	0.109	- 0.216	0.110
7	- 1.094	165.782	0.108	- 0.027	0.002	- 0.227	- 0.174	- 0.453	0.174	- 0.216	0.110
8	- 37.214	34.657	0.121	0.008	- 0.015	- 0.079	- 0.021	- 0.428	- 0.113	0.265	0.933
9	- 52.974	34.657	0.169	0.008	- 0.015	- 0.079	- 0.021	- 0.428	- 0.113	0.231	1.226
10	- 42.901	34.657	0.147	0.008	- 0.015	- 0.079	- 0.021	- 0.428	- 0.113	0.231	0.907
11	- 49.467	34.657	0.158	0.008	- 0.015	- 0.079	- 0.021	- 0.428	- 0.113	0.223	0.842
12	- 10.520	34.657	0.051	0.020	- 0.015	- 0.049	- 0.021	- 0.428	- 0.136	0.170	0.572
13	90.862	56.318	- 0.014	-	- 0.069	- 0.149	- 0.021	- 0.428	- 0.129	0.178	0.250

$$\begin{pmatrix} -0.144 & -0.390 & 2.053 & 0.207 & -1.147 & 1.265 & 0.447 & -1.832 & 1.663 & 0.992 & 0.329 \\ 0.999 & 0.675 & 2.760 & 5.033 & 2.172 & 0.803 & -1.246 & -1.846 & -0.485 & 6.039 & 2.975 \\ 1.807 & 2.558 & 3.832 & 4.165 & 3.128 & -0.689 & -1.106 & 1.903 & 0.817 & -19.790 & -20.129 \\ 2.052 & 3.892 & 0.122 & 3.756 & -0.502 & 0.365 & -3.831 & -0.803 & -0.115 & -0.060 & -5.519 \\ -0.514 & -1.050 & -3.541 & 5.953 & -0.183 & 0.415 & -4.354 & -4.272 & -0.223 & 7.500 & 2.440 \\ -0.818 & 1.954 & 5.421 & 5.098 & 3.475 & 1.076 & 3.667 & 2.731 & 3.119 & -1.419 & -3.341 \end{pmatrix} \times \begin{pmatrix} (l/b) \\ (B) \\ (FA) \\ (CA) \\ (SH) \\ (SS) \\ (M) \\ (SS/SH) \\ (NS) \\ (T) \\ (A) \\ 1 \end{pmatrix} = \begin{pmatrix} \alpha_1 \\ \alpha_2 \\ \alpha_3 \\ \alpha_4 \\ \alpha_5 \\ \alpha_6 \end{pmatrix}$$

7.5 M5P model

Figure 13 depicts the expected and observed CS of GPC mixtures adjusted with NS for the entire dataset. Similar to the other models, it was revealed that the l/b, SH content and M of the GPC mixtures, including NS have the largest influence on the CS, which coincides with previous experimental findings [60, 61]. Figure 14 shows the tree-shaped branch correlations. Also, the model (in Eq. (17)) parameters are summarized in Table 4, and the model variables will be selected based on the linear tree registration function.

$$\begin{aligned}
 CS = & \beta_1 + \beta_2\left(\frac{l}{b}\right) + \beta_3(b) + \beta_4(FA) + \beta_5(CA) + \beta_6(SH) \\
 & + \beta_7(SS) + \beta_8(M) + \beta_9\left(\frac{SS}{SH}\right) + \beta_{10}(NS) + \beta_{11}(T) \\
 & + \beta_{12}(A)
 \end{aligned} \tag{17}$$

For all of the training and testing datasets, there is a ± 25% error line. Furthermore, this model’s R, RMSE, OBJ and SI evaluation criteria are 0.955, 5.29 MPa, 5.42 MPa and 0.146, respectively, for the training datasets. This model is similar to the LR model regarding its application. The user can easily input its variables in the equation proposed above to predict the CS of GPC modified with NS.

Fig. 15 Comparison between model predictions of CS of GPC mixtures incorporated nS using testing datasets

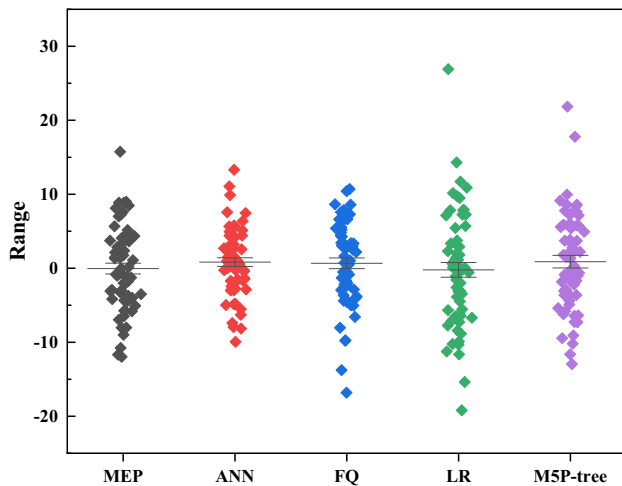
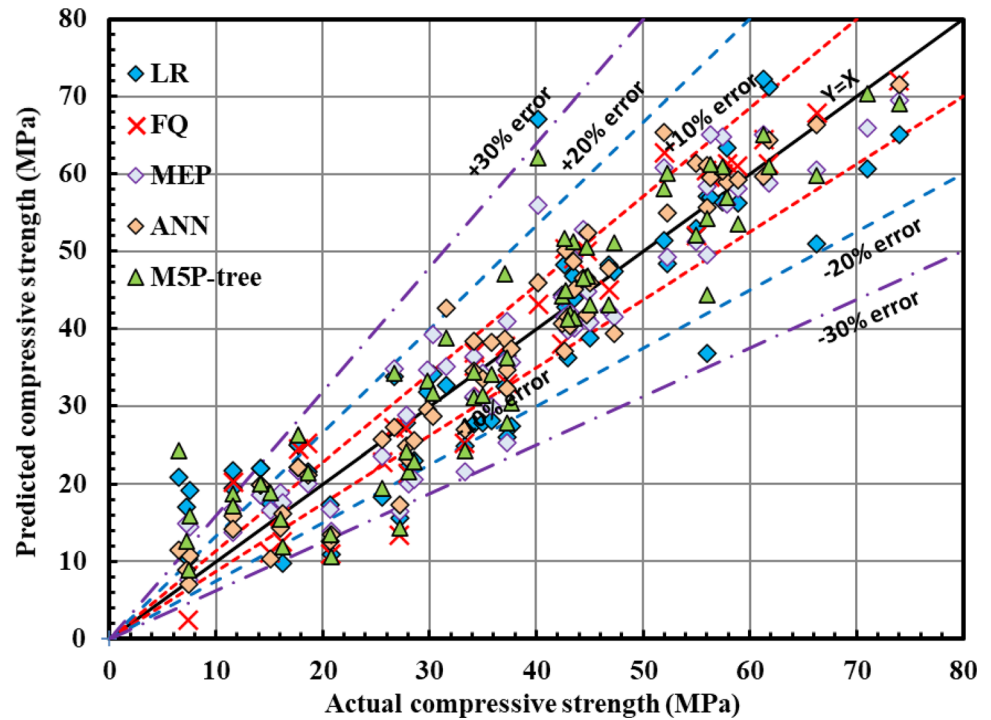


Fig. 16 Scatter interval for residual errors of the developed models

8 Model assessments

As previously stated, the effectiveness of the created models was assessed using four statistical tools: RMSE, SI, OBJ and R. In comparison with the LR, MEP, FQ and M5P models, the ANN model has a higher R, lower RMSE and lower OBJ and SI values.

The proposed models are compared based on the connection between predicted and actual CS for the training and testing datasets; the ANN model exhibited less variance; and the plotted data are close to the $Y = X$ line, indicating a small error in projected values. Figure 15 also

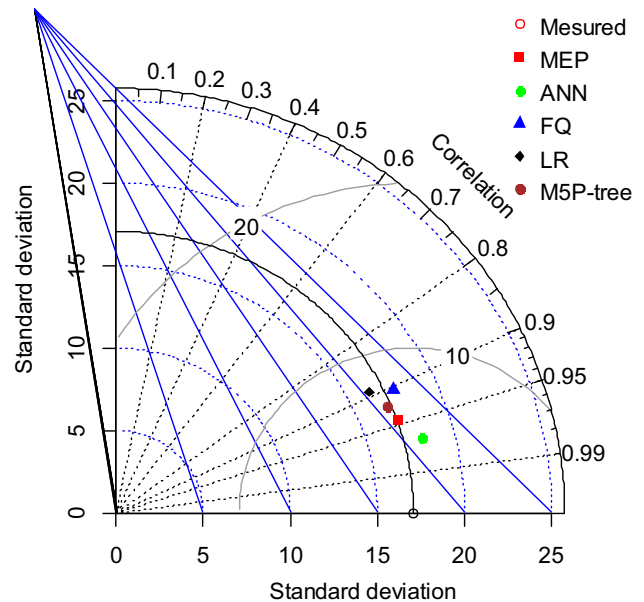


Fig. 17 Taylor diagram for comparing the developed models based on standard deviation and correlation coefficient for testing datasets

compares model predictions of the CS of GPC based on testing datasets. Figure 8 depicts the normalized predicted CS/actual CS versus the number of datasets for each model, while Fig. 16 illustrates the scatter interval for residual errors of the developed models. Figures (8, 15 and 16) show that the ANN model’s predicted and actual compressive strength values are close, indicating that the ANN model performs better than other models.

Figure 6 shows the OBJ values for all proposed models. The values for OBJ for LR, MEP, FQ, ANN and M5P are 7.91, 5.44, 4.25, 2.48 and 5.42, correspondingly. Compared to the LR, MEP, FQ and M5P models, the OBJ value of the ANN model is 219%, 119%, 71.4% and 118.5% lower, which emphasizes that this ANN model is superior for forecasting the compressive strength of GPC mixes.

Figure 7 presents the SI assessment parameter values for the proposed models during the training and testing phases. Based on this statistical evaluation tool, the accuracy of the ANN model for the training dataset was excellent, whereas the accuracy of the MEP, FQ and M5P models are in a good situation, while the performance of the LR model is in the fair condition; these results also demonstrated that the ANN model is more effective and performed better than LR, MEP, FQ and M5P for predicting the CS of GPC modified with NS.

In addition, as depicted in Fig. 17, Taylor diagrams are a graphical depiction of the degree to which a pattern (or

group of patterns) matches observations. Using their correlation, centered root-mean-square difference and variation amplitude, the similarity between the two patterns is determined (represented by their standard deviations). These diagrams are useful for evaluating multiple facets of complex models and comparing the relative competence of multiple models.

9 Sensitivity analysis

For the constructed models, a sensitivity analysis was undertaken to identify and examine the most impacting variable that affects the CS [25, 46]. The model’s reaction to changes in the input values provides insight into the model’s performance and, therefore, its potential to reflect reality. A single variable was retrieved from the training data, and the model was trained; the RMSE was also reported. The deleted variable in the trail with the highest RMSE has the most impact on CS prediction. The proportion of model parameter contribution is then calculated. The sensitivity evaluation result based on ANN and M5P-tree models is presented in Fig. 18a and b. The results suggest that the concrete ages are the most important and influential variable for CS prediction.

10 Conclusions

Distinct soft computing techniques can be utilized to construct accurate models; in this study, four different approaches were used to establish a trustworthy model for the prediction of compressive strength of GPC modified with NS; the key conclusions are as follows:

1. According to the data obtained, the largest amount of NS utilized by scholars in GPC mixtures was 60 kg/m³, while the average amount used was 11.65 kg/m³, which is approximately 3% of the amount of binder.
2. According to statistical evaluation tools, the ANN model predicts compressive strength more accurately than the LR, MEP, FQ and M5P-tree models. The projected compressive strength is less variable than the actual compressive strength.
3. Based on the results of the scatter index (SI) value, the performance of the ANN model is excellent, while the accuracy of the MEP, FQ and M5P is good; however, the LR model has a fair condition to predict the compressive strength of GPC modified with nano-silica.
4. The objective value (OBJ) for the ANN model is 2.48 MPa, which is 219%, 119%, 71.4% and 118.5% lower than the OBJ value of the LR, MEP, FQ and

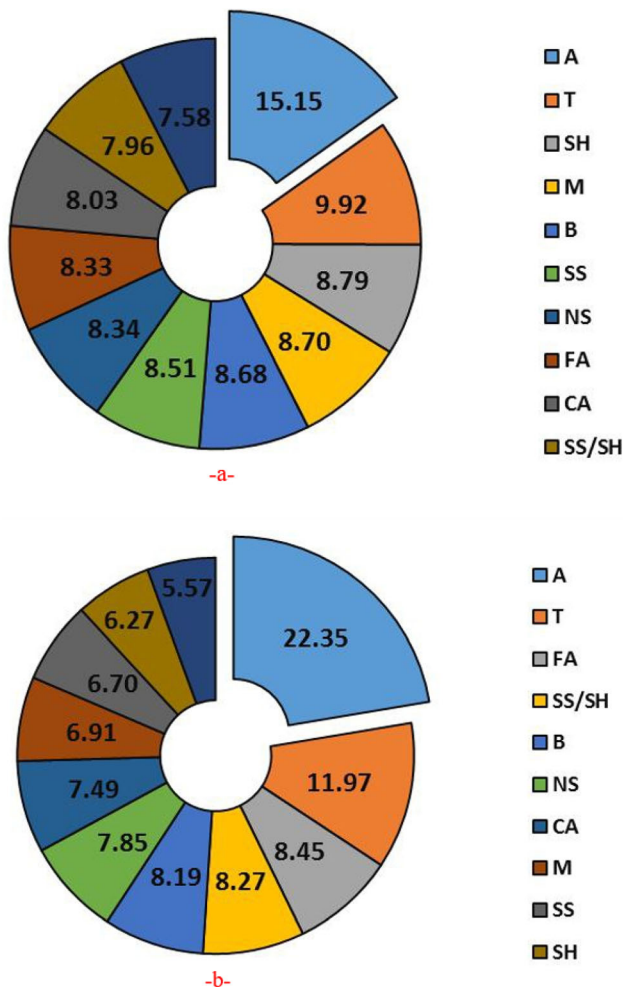


Fig. 18 Contribution of the model parameters in predicting the CS of GPC mixtures based on: a: M5P-tree model; b: ANN model

M5P-tree models, respectively, which improves the higher efficiency of the ANN model compared to the other models.

5. ANN, FQ, M5P, MEP and LR are the proposed models in ascending order of suitability and performance superiority for predicting the compressive strength of geopolymer concrete modified with nano-silica.
6. Depending on the outcome of the sensitivity analysis, the GPC specimen ages of the sample is the most relevant parameter on the compressive strength of GPC modified with nano-silica.
7. For estimating the CS of GPC mixtures modified by NS, a one-layer ANN structure network with six neurons is the optimal model combination.
8. Results indicate that the ratio of alkaline solution to the binder, the ratio of sodium silicate to sodium hydroxide, the molarity of sodium hydroxide and the ages of GPC specimens are the most influential variable parameters for predicting the compressive strength of GPC mixes modified with NS.
9. To diminish the limitations of the proposed models, the users can efficiently use the equations and models proposed with the same variables used in this study to train the models.

11 Recommendations

Based on the work that has been carried out in this study on the use of different modeling techniques to forecast the compressive strength of geopolymer concrete modified with nano-silica, the scope and gaps for further studies have been discussed and highlighted in the following:

- (a) Use of some modern techniques like dimensional analysis to reduce the number of input variable parameters.
- (b) Developing empirical models to predict the compressive strength of geopolymer concrete composites by considering other types of nano-materials like nano-alumina and nano-clay.
- (c) Using these model techniques to propose empirical equations for other mechanical properties of geopolymer concrete composites like splitting tensile strength, flexural strength and modulus of elasticity.
- (d) Conducting laboratory experiments to validate the developed models
- (e) Take benefits from these models and other intelligence techniques to standardize the mix design of geopolymer concrete composites just like traditional concrete.

Author contributions HUA was responsible for conceptualization and investigation; HUA, AAM, RHF, ASM., AAA, SMAQ and NHS were involved in methodology, software, data curation, writing—reviewing and editing, writing—original draft preparation and visualization; AAM, RHF, ASM, AAA, SMAQ and NHS participated in validation; HUA, AAM and ASM took part in formal analysis and project administration; AAA contributed to resources; and AAM and ASM were responsible for supervision. All authors have read and agreed to the published version of the manuscript.

Data availability All data generated or analyzed during this study are included in this published article.

Declarations

Conflict of interest We wish to confirm that there are no known conflicts of interest associated with this publication, and there has been no significant financial support for this work that could have influenced its outcome.

References

1. Ahmed HU, Mahmood LJ, Muhammad MA, Faraj RH, Qaidi SM, Sor NH, Mohammed AA (2022) Geopolymer concrete as a cleaner construction material: an overview on materials and structural performances. *Cleaner Mater* 5:100111. <https://doi.org/10.1016/j.clema.2022.100111>
2. Faraj RH, Ahmed HU, Sherwani AFH (2022) Fresh and mechanical properties of concrete made with recycled plastic aggregates. Woodhead Publishing, In Handbook of sustainable concrete and industrial waste management, pp 167–185. <https://doi.org/10.1016/B978-0-12-821730-6.00023-1>
3. Qaidi SM, Tayeh BA, Ahmed HU, Emad W (2022) A review of the sustainable utilisation of red mud and fly ash for the production of geopolymer composites. *Constr Build Mater* 350:128892. <https://doi.org/10.1016/j.conbuildmat.2022.128892>
4. Hamah Sor N, Hilal N, Faraj RH, Ahmed HU, Sherwani AFH (2021) Experimental and empirical evaluation of strength for sustainable lightweight self-compacting concrete by recycling high volume of industrial waste materials. *Eur J Environ Civ Eng* 26(15):7443–7460
5. Yildirim G, Sahmaran M, Ahmed HU (2015) Influence of hydrated lime addition on the self-healing capability of high-volume fly ash incorporated cementitious composites. *J Mater Civ Eng* 27(6):04014187. [https://doi.org/10.1061/\(ASCE\)MT.1943-5533.0001145](https://doi.org/10.1061/(ASCE)MT.1943-5533.0001145)
6. Sor NH, Ali TKM, Vali KS, Ahmed HU, Faraj RH, Bheel N, Mosavi A (2022) The behavior of sustainable self-compacting concrete reinforced with low-density waste Polyethylene fiber. *Mater Res Express* 9(3):035501. <https://doi.org/10.1088/2053-1591/ac58e8>
7. Sharif HH (2021) Fresh and mechanical characteristics of eco-efficient geopolymer concrete incorporating nano-silica: an overview. *Kurd J Appl Res.* <https://doi.org/10.24017/science.2021.2.6>
8. Qaidi SM, Tayeh BA, Isleem HF, de Azevedo AR, Ahmed HU, Emad W (2022) Sustainable utilization of red mud waste (bauxite residue) and slag for the production of geopolymer composites: a review. *Case Stud Constr Mater* 16:e00994. <https://doi.org/10.1016/j.cscm.2022.e00994>
9. Qaidi SM, Tayeh BA, Zeyad AM, de Azevedo AR, Ahmed HU, Emad W (2022) Recycling of mine tailings for the geopolymers

- production: a systematic review. *Case Studies Constr Mater* 16:e00933. <https://doi.org/10.1016/j.cscm.2022.e00933>
10. Ahmed HU, Mohammed AA, Rafiq S, Mohammed AS, Mosavi A, Sor NH, Qaidi S (2021) Compressive strength of sustainable geopolymers concrete composites: a state-of-the-art review. *Sustainability* 13(24):13502. <https://doi.org/10.3390/su132413502>
 11. Qaidi S, Najm HM, Abed SM, Ahmed HU, Dughaisi HA, Lawati JA, Sabri MM, Alkhatib F, Milad A (2022) Fly ash-based geopolymer composites: a review of the compressive strength and microstructure analysis. *Materials* 15(20):7098. <https://doi.org/10.3390/ma15207098>
 12. Mohammed AA, Ahmed HU, Mosavi A (2021) Survey of mechanical properties of geopolymer concrete: a comprehensive review and data analysis. *Materials* 14(16):4690. <https://doi.org/10.3390/ma14164690>
 13. Ahmed HU, Mohammed AA, Mohammad AS (2022) The role of nanomaterials in geopolymer concrete composites: a state-of-the-art review. *J Build Eng* 49:104062. <https://doi.org/10.1016/j.jobe.2022.104062>
 14. Faraj RH, Ahmed HU, Rafiq S, Sor NH, Ibrahim DF, Qaidi SM (2022) Performance of self-compacting mortars modified with nanoparticles: a systematic review and modeling. *Cleaner Mater* 4:100086. <https://doi.org/10.1016/j.clema.2022.100086>
 15. Assaedi H, Shaikh FUA, Low IM (2016) Influence of mixing methods of nano silica on the microstructural and mechanical properties of flax fabric reinforced geopolymer composites. *Constr Build Mater* 123:541–552. <https://doi.org/10.1016/j.conbuildmat.2016.07.049>
 16. Wiesner, M. R., & Bottero, J. Y. (2017). *Environmental nanotechnology: applications and impacts of nanomaterials*. McGraw-Hill Education. <https://www.accessengineeringlibrary.com/content/book/9780071828444>
 17. Adak D, Sarkar M, Mandal S (2017) Structural performance of nano-silica modified fly-ash based geopolymer concrete. *Constr Build Mater* 135:430–439. <https://doi.org/10.1016/j.conbuildmat.2016.12.111>
 18. Ahmed HU, Faraj RH, Hilal N, Mohammed AA, Sherwani AFH (2021) Use of recycled fibers in concrete composites: a systematic comprehensive review. *Compos Part B: Eng* 215:108769. <https://doi.org/10.1016/j.compositesb.2021.108769>
 19. Ahmed HU, Mostafa RR, Mohammed A, Sihag P, Qadir A (2022) Support vector regression (SVR) and grey wolf optimization (GWO) to predict the compressive strength of GGBFS-based geopolymer concrete. *Neural Comput Appl*. <https://doi.org/10.1007/s00521-022-07724-1>
 20. Faraj RH, Mohammed AA, Omer KM, Ahmed HU (2022) Soft computing techniques to predict the compressive strength of green self-compacting concrete incorporating recycled plastic aggregates and industrial waste ashes. *Clean Techn Environ Policy*. <https://doi.org/10.1007/s10098-022-02318-w>
 21. Ghafor K, Ahmed HU, Faraj RH, Mohammed AS, Kurda R, Qadir WS, Abdalla AA (2022) Computing models to predict the compressive strength of engineered cementitious composites (ECC) at various mix proportions. *Sustainability* 14(19):12876. <https://doi.org/10.3390/su141912876>
 22. Gao W, Karbasi M, Derakhsh AM, Jalili A (2019) Development of a novel soft-computing framework for the simulation aims: a case study. *Engineering with Computers* 35(1):315–322. <https://doi.org/10.1007/s00366-018-0601-y>
 23. Bilir T, Gencil O, Topcu IB (2016) Prediction of restrained shrinkage crack widths of slag mortar composites by Takagi and Sugeno ANFIS models. *Neural Comput Appl* 27(8):2523–2536. <https://doi.org/10.1007/s00521-015-2022-9>
 24. Behnood A, Daneshvar D (2020) A machine learning study of the dynamic modulus of asphalt concretes: an application of M5P model tree algorithm. *Constr Build Mater* 262:120544. <https://doi.org/10.1016/j.conbuildmat.2020.120544>
 25. Ahmed HU, Mohammed AS, Mohammed AA, Faraj RH (2021) Systematic multiscale models to predict the compressive strength of fly ash-based geopolymer concrete at various mixture proportions and curing regimes. *PLoS ONE* 16(6):e0253006. <https://doi.org/10.1371/journal.pone.0253006>
 26. Ahmed HU, Abdalla AA, Mohammed AS, Mohammed AA (2022) Mathematical modeling techniques to predict the compressive strength of high-strength concrete incorporated meta-kaolin with multiple mix proportions. *Cleaner Mater* 5:100132. <https://doi.org/10.1016/j.clema.2022.100132>
 27. Shahrajabian F, Behfarnia K (2018) The effects of nano particles on freeze and thaw resistance of alkali-activated slag concrete. *Constr Build Mater* 176:172–178. <https://doi.org/10.1016/j.conbuildmat.2018.05.033>
 28. Rabiaa E, Mohamed RAS, Sofi WH, Tawfik TA (2020) Developing geopolymer concrete properties by using nanomaterials and steel fibers. *Adv Mater Sci Eng* 2020:1–2. <https://doi.org/10.1155/2020/5186091>
 29. Mustakim SM, Das SK, Mishra J, Aftab A, Alomayri TS, Assaedi HS, Kaze CR (2020) Improvement in fresh, mechanical and microstructural properties of fly ash-blast furnace slag based geopolymer concrete by addition of nano and micro silica. *SILICON* 13:2415–2428. <https://doi.org/10.1007/s12633-020-00593-0>
 30. Çevik A, Alzebaree R, Humur G, Niş A, Gülşan ME (2018) Effect of nano-silica on the chemical durability and mechanical performance of fly ash based geopolymer concrete. *Ceram Int* 44(11):12253–12264. <https://doi.org/10.1016/j.ceramint.2018.04.009>
 31. Behfarnia K, Rostami M (2017) Effects of micro and nanoparticles of SiO₂ on the permeability of alkali activated slag concrete. *Constr Build Mater* 131:205–213. <https://doi.org/10.1016/j.conbuildmat.2016.11.070>
 32. Nuaklong, P., Jongvivatsakul, P., Pothisiri, T., Sata, V., & Chindaprasirt, P. (2020). Influence of rice husk ash on mechanical properties and fire resistance of recycled aggregate high-calcium fly ash geopolymer concrete. *Journal of Cleaner Production*, 252, 119797. <https://doi.org/10.1016/j.jclepro.2019.119797>
 33. Patel Y, Patel IN, Shah MJ (2015) Experimental investigation on compressive strength and durability properties of geopolymer concrete incorporating with nano silica. *Int J Civ Eng Technol* 6(5):135–143
 34. Ibrahim M, Johari MAM, Maslehuddin M, Rahman MK (2018) Influence of nano-SiO₂ on the strength and microstructure of natural pozzolan based alkali activated concrete. *Constr Build Mater* 173:573–585. <https://doi.org/10.1016/j.conbuildmat.2018.04.051>
 35. Mahboubi B, Guo Z, Wu H (2019) Evaluation of durability behavior of geopolymer concrete containing Nano-silica and Nano-clay additives in acidic media. *J civ Eng Mater Appl* 3(3):163–171. <https://doi.org/10.22034/JCEMA.2019.95839>
 36. Naskar S, Chakraborty AK (2016) Effect of nano materials in geopolymer concrete. *Perspect Sci* 8:273–275. <https://doi.org/10.1016/j.pisc.2016.04.049>
 37. Nuaklong P, Sata V, Wongsa A, Srinavin K, Chindaprasirt P (2018) Recycled aggregate high calcium fly ash geopolymer concrete with inclusion of OPC and nano-SiO₂. *Constr Build Mater* 174:244–252. <https://doi.org/10.1016/j.conbuildmat.2018.04.123>
 38. Vyas S, Mohammad S, Pal S, Singh N (2020) Strength and durability performance of fly ash based geopolymer concrete using nano silica. *Int J Eng Sci Technol* 4(2):1–12. <https://doi.org/10.29121/ijost.v4.i2.2020.73>

39. Etemadi, M., Pouraghajan, M., & Gharavi, H. (2020). Investigating the effect of rubber powder and nano silica on the durability and strength characteristics of geopolymeric concretes. *Journal of civil Engineering and Materials Application*, 4(4), 243–252. <https://doi.org/10.22034/jcema.2020.119979>
40. Angelin Lincy G, Velkennedy R (2020) Experimental optimization of metakaolin and nanosilica composite for geopolymer concrete paver blocks. *Struct Concr*. <https://doi.org/10.1002/suco.201900555>
41. Saini G, Vattipalli U (2020) Assessing properties of alkali activated GGBS based self-compacting geopolymer concrete using nano-silica. *Case Stud Constr Mater* 12:e00352. <https://doi.org/10.1016/j.cscm.2020.e00352>
42. Ibrahim M, Johari MAM, Rahman MK, Maslehuddin M, Mohamed HD (2018) Enhancing the engineering properties and microstructure of room temperature cured alkali activated natural pozzolan based concrete utilizing nanosilica. *Constr Build Mater* 189:352–365. <https://doi.org/10.1016/j.conbuildmat.2018.08.166>
43. Their JM, Özakça M (2018) Developing geopolymer concrete by using cold-bonded fly ash aggregate, nano-silica, and steel fiber. *Constr Build Mater* 180:12–22. <https://doi.org/10.1016/j.conbuildmat.2018.05.274>
44. Ibrahim M, Rahman MK, Johari MAM, Maslehuddin M (2018) Effect of Incorporating Nano-silica on the Strength of Natural Pozzolan-Based Alkali-Activated Concrete. In *International Congress on Polymers in Concrete* Springer, Cham, pp 703–709. https://doi.org/10.1007/978-3-319-78175-4_90
45. Ahmed HU, Mohammed AA, Mohammed A (2022) Soft computing models to predict the compressive strength of GGBS/FA-geopolymer concrete. *PLoS ONE* 17(5):e0265846. <https://doi.org/10.1371/journal.pone.0265846>
46. Faraj RH, Mohammed AA, Mohammed A, Omer KM, Ahmed HU (2021) Systematic multiscale models to predict the compressive strength of self-compacting concretes modified with nanosilica at different curing ages. *Eng Comput* 1–24:2365–2388. <https://doi.org/10.1007/s00366-021-01385-9>
47. Ahmed HU, Abdalla AA, Mohammed AS, Mohammed AA, Mosavi A (2022) Statistical Methods for Modeling the Compressive Strength of Geopolymer Mortar. *Materials* 15:1868. <https://doi.org/10.3390/ma15051868>
48. Holland, J. H. (1992). *Adaptation in natural and artificial systems: an introductory analysis with applications to biology, control, and artificial intelligence*. MIT press.
49. Jiang H, Mohammed AS, Kazeroon RA, Sarir P (2021) Use of the gene-expression programming equation and FEM for the high-strength CFST columns. *Appl Sci* 11(21):10468. <https://doi.org/10.3390/app112110468>
50. Asteris PG, Apostolopoulou M, Armaghani DJ, Cavaleri L, Chountalas AT, Guney D, Nguyen H (2020) On the metaheuristic models for the prediction of cement-metakaolin mortars compressive strength. *Metaheuristic Comput Appl* 1(1):063. <https://doi.org/10.12989/mca.2020.1.1.063>
51. Wang ML, Ramakrishnan V (1990) Evaluation of blended cement, mortar and concrete made from type III cement and kiln dust. *Constr Build Mater* 4(2):78–85. [https://doi.org/10.1016/0950-0618\(90\)90005-L](https://doi.org/10.1016/0950-0618(90)90005-L)
52. Sihag P, Jain P, Kumar M (2018) Modelling of impact of water quality on recharging rate of storm water filter system using various kernel function based regression. *Model Earth Syst Environ* 4(1):61–68. <https://doi.org/10.1007/s40808-017-0410-0>
53. Golareshani EM, Behnood A (2018) Application of soft computing methods for predicting the elastic modulus of recycled aggregate concrete. *J Clean Prod* 176:1163–1176. <https://doi.org/10.1016/j.jclepro.2017.11.186>
54. Demircan E, Harendra S, Vipulanandan C (2011) Artificial neural network and nonlinear models for gelling time and maximum curing temperature rise in polymer grouts. *J Mater Civ Eng* 23(4):372–377. [https://doi.org/10.1061/\(ASCE\)MT.1943-5533.0000172](https://doi.org/10.1061/(ASCE)MT.1943-5533.0000172)
55. Ahmed HU, Mohammed AS, Mohammed AA (2022) Multi-variable models including artificial neural network and M5P-tree to forecast the stress at the failure of alkali-activated concrete at ambient curing condition and various mixture proportions. *Neural Comput & Applic*. <https://doi.org/10.1007/s00521-022-07427-7>
56. Kocamaz AF, Ayaz Y, Karakoç MB, Türkmen İ, Demirboğa R (2021) Prediction of compressive strength and ultrasonic pulse velocity of admixed concrete using tree model M5P. *Struct Concr* 22:E800–E814. <https://doi.org/10.1002/suco.202000061>
57. Ahmed HU, Mohammed AS, Qaidi SMA, Faraj RH, Sor NH, Mohammed AA (2022) Compressive strength of geopolymer concrete composites: a systematic comprehensive review, analysis and modeling. *Eur J Environ Civ Eng*. <https://doi.org/10.1080/19648189.2022.2083022>
58. Oyebeisi S, Ede A, Olutoge F, Omole D (2020) Geopolymer concrete incorporating agro-industrial wastes: effects on mechanical properties microstructural behaviour and mineralogical phases. *Constr Build Mater* 256:119390. <https://doi.org/10.1016/j.conbuildmat.2020.119390>
59. Abdalla AA, Salih Mohammed A (2022) Theoretical models to evaluate the effect of SiO₂ and CaO contents on the long-term compressive strength of cement mortar modified with cement kiln dust (CKD). *Archives Civ Mech Eng* 22(3):1–21. <https://doi.org/10.1007/s43452-022-00418-4>
60. Ghafoor MT, Khan QS, Qazi AU, Sheikh MN, Hadi MNS (2021) Influence of alkaline activators on the mechanical properties of fly ash based geopolymer concrete cured at ambient temperature. *Constr Build Mater* 273:121752. <https://doi.org/10.1016/j.conbuildmat.2020.121752>
61. Aliabdo AA, Abd Elmoaty M, Salem HA (2016) Effect of water addition, plasticizer and alkaline solution constitution on fly ash based geopolymer concrete performance. *Constr Build Mater* 121:694–703. <https://doi.org/10.1016/j.conbuildmat.2016.06.062>

Publisher's Note Springer Nature remains neutral with regard to jurisdictional claims in published maps and institutional affiliations.

Springer Nature or its licensor (e.g. a society or other partner) holds exclusive rights to this article under a publishing agreement with the author(s) or other rightsholder(s); author self-archiving of the accepted manuscript version of this article is solely governed by the terms of such publishing agreement and applicable law.